Chapter 6

The Chaotic Motion of Dynamical Systems

19 March 2010

Adapted from *An Introduction to Computer Simulation Methods* by Harvey Gould, Jan Tobochnik, and Wolfgang Christian

We study simple nonlinear deterministic models that exhibit chaotic behavior. We will find that the use of the computer to do numerical experiments will help us gain insight into the nature of chaos.

6.1 Introduction to chaos

Most natural phenomena are intrinsically nonlinear. Weather patterns and the turbulent motion of fluids are everyday examples. Although we have explored some of the properties of nonlinear systems in Chapter 4, it is easier to introduce some of the important concepts in the context of ecology. Our first goal will be to motivate and analyze the one-dimensional difference equation

$$x_{n+1} = 4rx_n(1 - x_n), \tag{6.1}$$

where x_n is the ratio of the population in the nth generation to a reference population. We shall see that the dynamical properties of (6.1) are surprisingly intricate and have important implications for the development of a more general description of nonlinear phenomena. The significance of the behavior of (6.1) is indicated by the following quote from the ecologist Robert May:

> *"Its study does not involve as much conceptual sophistication as does elementary calculus. Such study would greatly enrich the student's intuition about nonlinear systems. Not only in research but also in the everyday world of politics and economics we would all be better off if more people realized that simple nonlinear systems do not necessarily possess simple dynamical properties."*

The study of chaos is of much current interest, but the phenomena is not new and has been of interest, particularly to astronomers and mathematicians, for over one hundred years. Much of the current interest is due to the use of the computer as a tool for making empirical observations. We will use the computer in this spirit.

6.2 A Simple One-Dimensional Map

Imagine an island with an insect population that breeds in the summer and leaves eggs that hatch the following spring. Because the population growth occurs at discrete times, it is appropriate to model the population growth by a difference equation rather than by a differential equation. A simple model of population growth that relates the population in generation $n+1$ to the population in generation n is given by

$$P_{n+1} = aP_n, \tag{6.2}$$

where P_n is the population in generation n and a is a constant. In the following, we will assume that the time interval between generations is unity, and will refer to n as the time.

If $a < 1$, the population decreases at each generation and eventually the population becomes extinct. If $a > 1$, each generation will be a times larger than the previous one. In this case (6.2) leads to geometrical growth and an unbounded population. Although the unbounded nature of geometrical growth is clear, it is remarkable that most of us do not integrate our understanding of geometrical growth into our everyday lives. Can a bank pay 4% interest each year indefinitely? Can the world's human population grow at a constant rate forever?

It is natural to formulate a more realistic model in which the population is bounded by the finite carrying capacity of its environment. A simple model of density-dependent growth is

$$P_{n+1} = P_n(a - bP_n). \tag{6.3}$$

Equation (6.3) is nonlinear due to the presence of the quadratic term in P_n. The linear term represents the natural growth of the population; the quadratic term represents a reduction of this natural growth caused, for example, by overcrowding or by the spread of disease.

It is convenient to rescale the population by letting $P_n = (a/b)x_n$ and rewriting (6.3) as

$$x_{n+1} = ax_n(1 - x_n). \tag{6.4}$$

The replacement of P_n by x_n changes the units used to define the various parameters. To write (6.4) in the standard form (6.1), we define the parameter $r = a/4$ and obtain

$$x_{n+1} = f(x_n) = 4rx_n(1 - x_n). \tag{6.5}$$

The rescaled form (6.5) has the desirable feature that its dynamics are determined by a single control parameter r instead of the two parameters a and b. Note that if $x_n > 1$, x_{n+1} will be negative. To avoid this unphysical feature, we impose the conditions that x is restricted to the interval $0 \le x \le 1$ and $0 < r \le 1$. Because the function $f(x)$ defined in (6.5) transforms any point on the one-dimensional interval $[0, 1]$ into another point in the same interval, the function f is called a *one-dimensional map.*

The form of $f(x)$ in (6.5) is known as the *logistic* map. The logistic map is a simple example of a *dynamical system*, that is, the map is a deterministic, mathematical prescription for finding the future state of a system given its present state.

The sequence of values x_0, x_1, x_2, ... is called the *trajectory*. To check your understanding, suppose that the initial value of x_0 or *seed* is $x_0 = 0.5$ and $r = 0.2$. Do a calculation to show that the trajectory is $x_1 = 0.2, x_2 = 0.128, x_3 = 0.089293, \ldots$ The first thirty iterations of (6.5) are shown for two values of r in Figure 6.1.

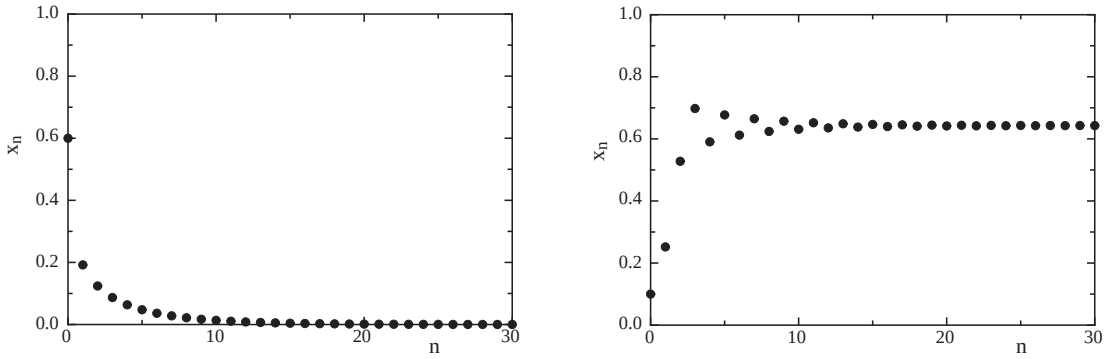

Figure 6.1: (a) The trajectory of x for $r = 0.2$ and $x_0 = 0.6$. The stable fixed point is at $x = 0$. (b) The trajectory for $r = 0.7$ and $x_0 = 0.1$. Note the initial transient behavior.

The Iterate model in this chapter's source code directory computes a table of values using a map such as (6.2) or (6.5).

Exercise 6.1. Iteration

An iterative method for calculating the square root x of a number a is based on the observation that $x = a/x$. If we guess the value of the root x and our guess is too small (large), then a/x will be too large (small) and the average $(x + a/x)/2$ will be closer to the true value. The true value of $\sqrt{a}$ can therefore be found by iterating

$$x_{n+1} = (x_n + a/x_n)/2. \tag{6.6}$$

Use the Iterate model to compute the square root of some representative numbers. Does the algorithm always converge regardless of the initial guess x_0? What happens if a is negative? ■

Problem 6.2. The trajectory of the logistic map

a. Modify the Iterate model to produce a plot of the trajectory to reproduce the results shown in Figure 6.1.

b. Use your modified model to explore the dynamical behavior of the logistic map in (6.5) with $r = 0.24$ for different values of x_0. Show numerically that $x = 0$ is a *stable fixed point* for this value of r. That is, the iterated values of x converge to $x = 0$ independently of the value of x_0. If x represents the population of insects, describe the qualitative behavior of the population.

c. Explore the dynamical behavior of (6.5) for $r = 0.26, 0.5, 0.74$, and 0.748. A fixed point is *unstable* if for almost all values of x_0 near the fixed point, the trajectories diverge from it. Verify that $x = 0$ is an unstable fixed point for $r > 0.25$. Show that for the suggested values of r, the iterated values of x do not change after an initial *transient*, that is, the long time dynamical behavior is *period* 1. In Appendix 6A we show that for $r < 3/4$ and for x_0 in the interval $0 < x_0 < 1$, the trajectories approach the *stable attractor* at $x = 1 - 1/4r$. The set of initial points that iterate to the attractor is called the *basin* of the attractor. For the logistic map, the interval $0 < x < 1$ is the basin of attraction of the attractor $x = 1 - 1/4r$.

d. Explore the dynamical properties of (6.5) for $r = 0.752$, 0.76, 0.8, and 0.862. For $r = 0.752$ and 0.862 approximately 1000 iterations are necessary to obtain convergent results. Show that if r is greater than 0.75, x oscillates between two values after an initial transient behavior. That is, instead of a stable cycle of period 1 corresponding to one fixed point, the system has a stable cycle of period 2. The value of r at which the single fixed point x^* splits or *bifurcates* into two values ${x_1}^*$ and ${x_2}^*$ is $r = b_1 = 3/4$. The pair of x values, ${x_1}^*$ and ${x_2}^*$, form a *stable attractor* of period 2.

e. What are the stable attractors of (6.5) for $r = 0.863$ and 0.88? What is the corresponding period? What are the stable attractors and corresponding periods for $r = 0.89$, 0.891, and 0.8922? ■

A more elegant and useful way to determine the behavior of (6.5) is to plot the long-term values of x as a function of r (see Figure 6.2). The Logistic Bifurcation model in this chapter's source directory plots the iterated values of x after the initial transient behavior is discarded. Such a plot is called a bifurcation diagram and is generated by Bifurcate model. For each value of r, the first `nTransient` values of x are computed but not plotted. Then the next `nPlot` values of x are plotted, with the first half in one color and the second half in another. This process is repeated for a new value of r during every evolution step until the desired range of r values is reached. The magnitude of `nPlot` should be at least as large as the longest period that you wish to observe.

Problem 6.3. Qualitative features of the logistic map

a. Use the Logistic Bifurcation model to identify period 2, period 4, and period 8 behavior as can be seen in Figure 6.2. Choose `nTransient` ≥ 1000. It might be necessary to "zoom in" on a portion of the plot. How many period doublings can you find?

b. Change the scale so that you can follow the iterations of x from period 4 to period 16 behavior. How does the plot look on this scale in comparison to the original scale?

c. Describe the shape of the trajectory near the bifurcations from period 2 to period 4, period 4 to 8, etc. These bifurcations are frequently called *pitchfork bifurcations*. ■

The bifurcation diagram in Figure 6.2 indicates that the period doubling behavior ends at $r \approx 0.892$. This value of r is known very precisely and is given by $r = r_\infty = 0.892486417967\ldots$ At $r = r_\infty$, the sequence of period doublings accumulate to a trajectory of infinite period. In Problem 6.4 we explore the behavior of the trajectories for $r > r_\infty$.

Problem 6.4. Chaotic behavior

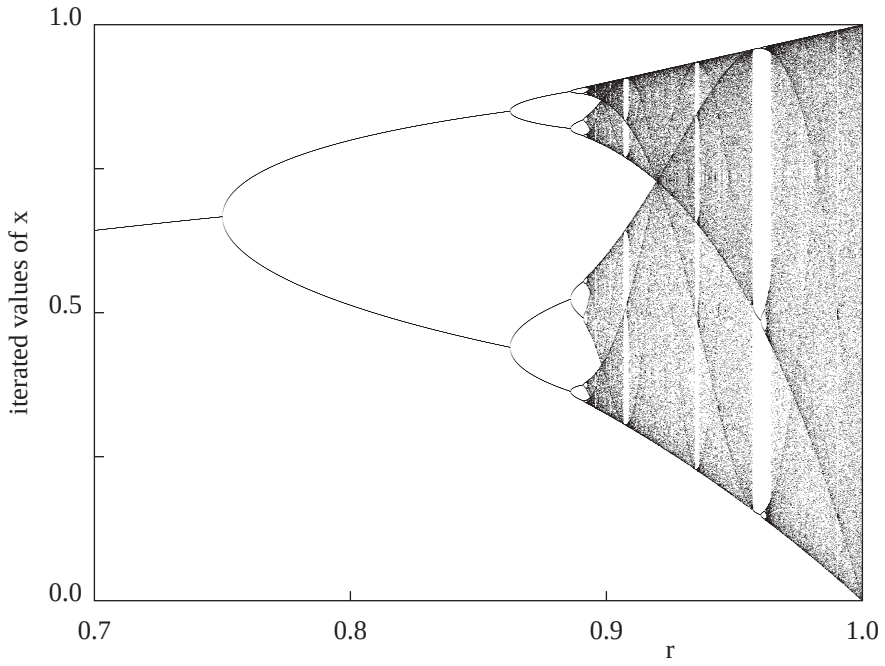

Figure 6.2: Bifurcation diagram of the logistic map. For each value of r, the iterated values of x_n are plotted after the first 1000 iterations are discarded. Note the transition from periodic to chaotic behavior and the narrow windows of periodic behavior within the region of chaos.

a. For $r > r_\infty$, two initial conditions that are very close to one another can yield very different trajectories after a few iterations. As an example, choose $r = 0.91$ and consider $x_0 = 0.5$ and 0.5001. How many iterations are necessary for the iterated values of x to differ by more than ten percent? What happens for $r = 0.88$ for the same choice of seeds?

b. The accuracy of floating point numbers retained on a digital computer is finite. To test the effect of the finite accuracy of your computer, choose $r = 0.91$ and $x_0 = 0.5$ and compute the trajectory for 200 iterations. Then modify your program so that after each iteration, the operation `x = x/10` is followed by `x = 10*x`. This combination of operations truncates the last digit that your computer retains. Compute the trajectory again and compare your results. Do you find the same discrepancy for $r < r_\infty$?

c. What are the dynamical properties for $r = 0.958$? Can you find other windows of periodic behavior in the interval $r_\infty < r < 1$? ■

6.3 Period Doubling

The results of the numerical experiments that we did in Section 6.2 probably have convinced you that the dynamical properties of a simple nonlinear deterministic system can be quite complicated.

To gain more insight into how the dynamical behavior depends on r, we introduce a simple graphical method for iterating (6.5). In Figure 6.3 we show a graph of $f(x)$ versus x for $r = 0.7$. A diagonal line corresponding to $y = x$ intersects the curve $y = f(x)$ at the two fixed points $x^* = 0$ and $x^* = 9/14 \approx 0.642857$ (see (6.7b)). If x_0 is not a fixed point, we can find the trajectory in the following way. Draw a vertical line from $(x = x_0, y = 0)$ to the intersection with the curve $y = f(x)$ at $(x_0, y_0 = f(x_0))$. Next draw a horizontal line from (x_0, y_0) to the intersection with the diagonal line at (y_0, y_0). On this diagonal line $y = x$, and hence the value of x at this intersection is the first iteration $x_1 = y_0$. The second iteration x_2 can be found in the same way. From the point (x_1, y_0), draw a vertical line to the intersection with the curve $y = f(x)$. Keep y fixed at $y = y_1 = f(x_1)$, and draw a horizontal line until it intersects the diagonal line; the value of x at this intersection is x_2. Further iterations can be found by repeating this process.

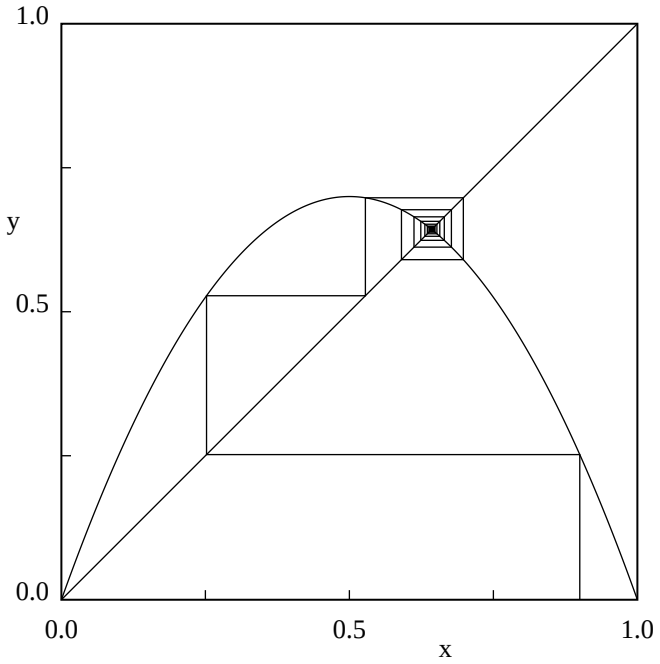

Figure 6.3: Graphical representation of the iteration of the logistic map (6.5) with $r = 0.7$ and $x_0 = 0.9$. Note that the graphical solution converges to the fixed point $x^* \approx 0.643$.

This graphical method is illustrated in Figure 6.3 for $r = 0.7$ and $x_0 = 0.9$. If we begin with any x_0 (except $x_0 = 0$ and $x_0 = 1$), the iterations will converge to the fixed point $x^* \approx 0.643$. It would be a good idea to repeat the procedure shown in Figure 6.3 by hand. For $r = 0.7$, the fixed point is stable (an attractor of period 1). In contrast, no matter how close x_0 is to the fixed point at $x = 0$, the iterates diverge away from it, and this fixed point is unstable.

How can we explain the qualitative difference between the fixed point at $x = 0$ and at $x^* = 0.642857$ for $r = 0.7$? The local slope of the curve $y = f(x)$ determines the distance moved horizontally each time f is iterated. A slope steeper than 45° leads to a value of x further away from its initial value. Hence, the criterion for the stability of a fixed point is that the magnitude

of the slope at the fixed point must be less than 45°. That is, if $|df(x)/dx|_{x=x^*}$ is less than unity, then x^* is stable; conversely, if $|df(x)/dx|_{x=x^*}$ is greater than unity, then x^* is unstable.

An inspection of $f(x)$ in Figure 6.3 shows that $x = 0$ is unstable because the slope of $f(x)$ at $x = 0$ is greater than unity. In contrast, the magnitude of the slope of $f(x)$ at $x = x^* \approx 0.643$ is less than unity and this fixed point is stable. In Appendix 6A, we show that

$$x^* = 0 \text{ is stable for } 0 < r < 1/4, \tag{6.7a}$$

and

$$x^* = 1 - \frac{1}{4r} \text{ is stable for } 1/4 < r < 3/4. \tag{6.7b}$$

Thus for $0 < r < 3/4$, the behavior after many iterations is known.

What happens if r is greater than $3/4$? We found in Section 6.2 that if r is slightly greater than $3/4$, the fixed point of f becomes unstable and bifurcates to a cycle of period 2. Now x returns to the same value after every second iteration, and the fixed points of $f\big(f(x)\big)$ are the stable attractors of $f(x)$. In the following, we write $f^{(2)}(x) = f\big(f(x)\big)$ and $f^{(n)}(x)$ for the nth iterate of $f(x)$. (Do not confuse $f^{(n)}(x)$ with the nth derivative of $f(x)$.) For example, the second iterate $f^{(2)}(x)$ is given by the fourth-order polynomial:

$$\begin{aligned} f^{(2)}(x) &= 4r\big[4rx(1-x)\big] - 4r\big[4rx(1-x)\big]^2 \\ &= 4r[4rx(1-x)]\big[1 - 4rx(1-x)\big] \\ &= 16r^2x\big[-4rx^3 + 8rx^2 - (1+4r)x + 1\big]. \end{aligned} \tag{6.8}$$

What happens if we increase r still further? Eventually the magnitude of the slope of the fixed points of $f^{(2)}(x)$ exceeds unity and the fixed points of $f^{(2)}(x)$ become unstable. Now the cycle of f is period 4, and the fixed points of the fourth iterate $f^{(4)}(x) = f^{(2)}\big(f^{(2)}(x)\big) = f\big(f\big(f(f(x))\big)\big)$ are stable. These fixed points also eventually become unstable, and we are led to the phenomena of *period doubling* that we observed in Problem 6.3.

The Logistic Cobweb model in the chapter's code directory implements the graphical analysis of the iterations of $f(x)$. The nth order iterates are defined using the *recursive* method `f(x,iterate)` shown in Listing 6.1. (The parameter `iterate` is 1, 2, and 4 for the functions $f(x)$, $f^{(2)}(x)$, and $f^{(4)}(x)$ respectively and the value of the control parameter is 0.8.) Recursion is an idea that is simple once you understand it, but it can be difficult to grasp initially. Although the method calls itself, the rules for method calls remain the same. Imagine that a recursive method is called. The computer then starts to execute the code in the method, but comes to another call of the same method as itself. At this point the computer stops executing the code of the original method, and makes an exact copy of the method with possibly different input parameters, and starts executing the code in the copy. There are now two possibilities. One is that the computer comes to the end of the copy without another recursive call. In that case the computer deletes the copy of the method and continues executing the code in the original method. The other possibility is that a recursive call is made in the copy, and a third copy is made of the method, and the code in the third copy is now executed. This process continues until the code in all the copies is executed. Every recursive method must have a possibility of reaching the end of the method; otherwise, the program will eventually crash.

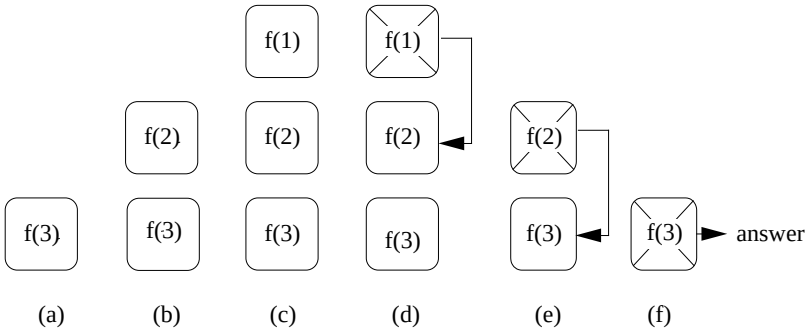

Figure 6.4: Example of the calculation of `f(0.4,3)` using the recursive function defined in the Logistic Cobweb model. The number in each box is the value of the variable `iterate`. The computer executes code from left to right, and each box represents a copy of the function in the computer's memory. The input values $x = 0.4$ and $r = 0.8$, which are the same in each copy, are not shown. The arrows indicate when a copy is finished and its value is returned to one of the other copies. Notice that the first copy of the function, $f(3)$, is the last one to finish. The value of `f(x,3)` $= 0.7842$.

Listing 6.1: The `f(x,iterate)` custom method evaluates the logistic function recursively.

```
public double f (double x, int iterate) {
  x=4*r*x*(1-x); // compute new x
  if(iterate==1) return x;
    else return f ( x, iterate-1);
}
```

To understand the method `f(x,iterate)`, suppose we want to compute `f(0.4,3)`. First we write `f(0.4,3)` as in Figure 6.4a. Follow the statements within the method until another call to `f(0.4,iterate)` occurs. In this case, the call is to `f(0.4,iterate-1)` which equals `f(0.4,2)`. Write `f(0.4,2)` above `f(0.4,3)` (see Figure 6.4b). When you come to the end of the definition of the method, write down the value of `f` that is actually returned, and remove the method from the stack by crossing it out (see Figure 6.4d). This returned value for `f` equals `y` if `iterate` > 1, or it is the value of the logistic function for `iterate` $= 1$. Continue deleting copies of `f` as they are finished, until there are no copies left on the paper. The final value of `f` is the value returned by the computer.

Exercise 6.5. Recursion

Create a simple model that defines the control parameter `r` and the `f(x,iterate)` custom method and prints the value of the input parameters `x` and `iterate` when the method is invoked. Test your method with `f(0.4,3)`. Is the answer the same as your hand calculation? ■

Problem 6.6. Qualitative properties of the fixed points

a. Use the Logistic Cobweb model to show graphically that there is a single stable fixed point of $f(x)$ for $r < 3/4$. It would be instructive to modify the program so that the value of the slope

$df/dx|_{x=x_n}$ is shown as you step each iteration. At what value of r does the absolute value of this slope exceed unity? Let b_1 denote the value of r at which the fixed point of $f(x)$ bifurcates and becomes unstable. Verify that $b_1 = 0.75$.

b. Describe the trajectory of $f(x)$ for $r = 0.785$. Is the fixed point given by $x = 1 - 1/4r$ stable or unstable? What is the nature of the trajectory if $x_0 = 1 - 1/4r$? What is the period of $f(x)$ for all other choices of x_0? What are the values of the two-point attractor?

c. The function $f(x)$ is symmetrical about $x = 1/2$ where $f(x)$ is a maximum. What are the qualitative features of the second iterate $f^{(2)}(x)$ for $r = 0.785$? Is $f^{(2)}(x)$ symmetrical about $x = 1/2$? For what value of x does $f^{(2)}(x)$ have a minimum? Iterate $x_{n+1} = f^{(2)}(x_n)$ for $r = 0.785$ and find its two fixed points ${x_1}^*$ and ${x_2}^*$. (Try $x_0 = 0.1$ and $x_0 = 0.3$.) Are the fixed points of $f^{(2)}(x)$ stable or unstable for this value of r? How do these values of ${x_1}^*$ and ${x_2}^*$ compare with the values of the two-point attractor of $f(x)$? Verify that the slopes of $f^{(2)}(x)$ at ${x_1}^*$ and ${x_2}^*$ are equal.

d. Verify the following properties of the fixed points of $f^{(2)}(x)$. As r is increased, the fixed points of $f^{(2)}(x)$ move apart and the slope of $f^{(2)}(x)$ at its fixed points decreases. What is the value of $r = s_2$ at which one of the two fixed points of $f^{(2)}$ equals $1/2$? What is the value of the other fixed point? What is the slope of $f^{(2)}(x)$ at $x = 1/2$? What is the slope at the other fixed point? As r is further increased, the slopes at the fixed points become negative. Finally at $r = b_2 \approx 0.8623$, the slopes at the two fixed points of $f^{(2)}(x)$ equal -1, and the two fixed points of $f^{(2)}$ become unstable. (The exact value of b_2 is $b_2 = (1 + \sqrt{6})/4$.)

e. Show that for r slightly greater than b_2, for example, $r = 0.87$, there are four stable fixed points of $f^{(4)}(x)$. What is the value of $r = s_3$ when one of the fixed points equals $1/2$? What are the values of the three other fixed points at $r = s_3$?

f. Determine the value of $r = b_3$ at which the four fixed points of $f^{(4)}$ become unstable.

g. Choose $r = s_3$ and determine the number of iterations that are necessary for the trajectory to converge to period 4 behavior. How does this number of iterations change when neighboring values of r are considered? Choose several values of x_0 so that your results do not depend on the initial conditions. ■

Problem 6.7. Periodic windows in the chaotic regime

a. If you look closely at the bifurcation diagram in Figure 6.2, you will see that the range of chaotic behavior for $r > r_\infty$ is interrupted by intervals of periodic behavior. Magnify your bifurcation diagram so that you can look at the interval $0.957107 \leq r \leq 0.960375$, where a periodic trajectory of period 3 occurs. (Period 3 behavior starts at $r = (1 + \sqrt{8})/4$.) What happens to the trajectory for slightly larger r, for example, $r = 0.9604$?

b. Plot $f^{(3)}(x)$ versus x at $r = 0.96$, a value of r in the period 3 window. Draw the line $y = x$ and determine the intersections with $f^{(3)}(x)$. The stable fixed points satisfy the condition $x^* = f^{(3)}(x^*)$. Because $f^{(3)}(x)$ is an eighth-order polynomial, there are eight solutions (including $x = 0$). Find the intersections of $f^{(3)}(x)$ with $y = x$ and identify the three stable fixed points. What are the slopes of $f^{(3)}(x)$ at these points? Then decrease r to $r = 0.957107$, the (approximate)

value of r below which the system is chaotic. Draw the line $y = x$ and determine the number of intersections with $f^{(3)}(x)$. Note that at this value of r, the curve $y = f^{(3)}(x)$ is tangent to the diagonal line at the three stable fixed points. For this reason, this type of transition is called a *tangent bifurcation*. Note that there also is an unstable point at $x \approx 0.76$.

c. Plot $x_{n+1} = f^{(3)}(x_n)$ versus n for $r = 0.9571$, a value of r just below the onset of period 3 behavior. How would you describe the behavior of the trajectory? This type of chaotic motion is an example of *intermittency*, that is, nearly periodic behavior interrupted by occasional irregular bursts.

d. To understand the mechanism for the intermittent behavior, we need to "zoom in" on the values of x near the stable fixed points that you found in part (c). To do so change the scale of the plot. You will see a narrow channel between the diagonal line $y = x$ and the plot of $f^{(3)}(x)$ near each fixed point. The trajectory can require many iterations to squeeze through the channel, and we see apparent period 3 behavior during this time. Eventually, the trajectory escapes from the channel and bounces around until it is again enters a channel at some unpredictable later time. ■

6.4 Universal Properties and Self-Similarity

In Sections 6.2 and 6.12 we found that the trajectory of the logistic map has remarkable properties as a function of the control parameter r. In particular, we found a sequence of period doublings accumulating in a chaotic trajectory of infinite period at $r = r_\infty$. For most values of $r > r_\infty$, the trajectory is very sensitive to the initial conditions. We also found "windows" of period 3, 6, 12, ... embedded in the range of chaotic behavior. How typical is this type of behavior? In the following, we will find further numerical evidence that the general behavior of the logistic map is independent of the details of the form (6.5) of $f(x)$.

You might have noticed that the range of r between successive bifurcations becomes smaller as the period increases (see Table 6.1). For example, $b_2 - b_1 = 0.112398$, $b_3 - b_2 = 0.023624$, and $b_4 - b_3 = 0.00508$. A good guess is that the decrease in $b_k - b_{k-1}$ is geometric, that is, the ratio $(b_k - b_{k-1})/(b_{k+1} - b_k)$ is a constant. You can check that this ratio is not exactly constant, but converges to a constant with increasing k. This behavior suggests that the sequence of values of b_k has a limit and follows a geometrical progression:

$$b_k \approx r_\infty - C\,\delta^{-k}, \tag{6.9}$$

where δ is known as the *Feigenbaum number* and C os a constant. From (6.9) it is easy to show that δ is given by the ratio

$$\delta = \lim_{k\to\infty} \frac{b_k - b_{k-1}}{b_{k+1} - b_k}. \tag{6.10}$$

Problem 6.8. Estimation of the Feigenbaum constant

a. Derive the relation (6.10) given (6.9). Plot $\delta_k = (b_k - b_{k-1})/(b_{k+1} - b_k)$ versus k using the values of b_k in Table 6.1 and determine the value of δ. Are the number of decimal places given

k	b_k
1	0.750 000
2	0.862 372
3	0.886 023
4	0.891 102
5	0.892 190
6	0.892 423
7	0.892 473
8	0.892 484

Table 6.1: Values of the control parameter $r = b_k$ for the onset of the kth bifurcation. Six decimal places are shown.

in Table 6.1 for b_k sufficient for all the values of k shown? The best numerical determination of δ is

$$\delta = 4.669\,201\,609\,102\,991\ldots \tag{6.11}$$

The number of decimal places in (6.11) is shown to indicate that δ is known precisely. Use (6.9) and (6.11) and the values of b_k to determine the value of r_∞.

b. In Problem 6.6 we found that one of the four fixed points of $f^{(4)}(x)$ is at $x^* = 1/2$ for $r = s_3 \approx 0.87464$. We also found that the convergence to the fixed points of $f^{(4)}(x)$ for this value of r is more rapid than at nearby values of r. In Appendix 6A we show that these *superstable* trajectories occur whenever one of the fixed points is at $x^* = 1/2$. The values of $r = s_m$ that give superstable trajectories of period 2^{m-1} are much better defined than the points of bifurcation, $r = b_k$. The rapid convergence to the final trajectories also gives better numerical results, and we always know one member of the trajectory, namely $x = 1/2$. Assume that δ can be defined as in (6.10) with b_k replaced by s_m. Use $s_1 = 0.5$, $s_2 \approx 0.809017$, and $s_3 = 0.874640$ to determine δ. The numerical values of s_m are found in Project 6.16 by solving the equation $f^{(m)}(x = 1/2) = 1/2$ numerically; the first eight values of s_m are listed in Table 6.2 in Section 6.11. ■

We can associate another number with the series of "pitchfork" bifurcations. From Figures 6.3 and 6.5 we see that each pitchfork bifurcation gives birth to "twins" with the new generation more densely packed than the previous generation. One measure of this density is the maximum distance M_k between the values of x describing the bifurcation (see Figure 6.5). The disadvantage of using M_k is that the transient behavior of the trajectory is very long at the boundary between two different periodic behaviors. A more convenient measure of the distance is the quantity $d_k = {x_k}^* - 1/2$, where ${x_k}^*$ is the value of the fixed point nearest to the fixed point $x^* = 1/2$. The first two values of d_k are shown in Figure 6.6 with $d_1 \approx 0.3090$ and $d_2 \approx -0.1164$. The next value is $d_3 \approx 0.0460$. Note that the fixed point nearest to $x = 1/2$ alternates from one side of $x = 1/2$ to the other. We define the quantity α by the ratio

$$\alpha = \lim_{k\to\infty} -\Big(\frac{d_k}{d_{k+1}}\Big). \tag{6.12}$$

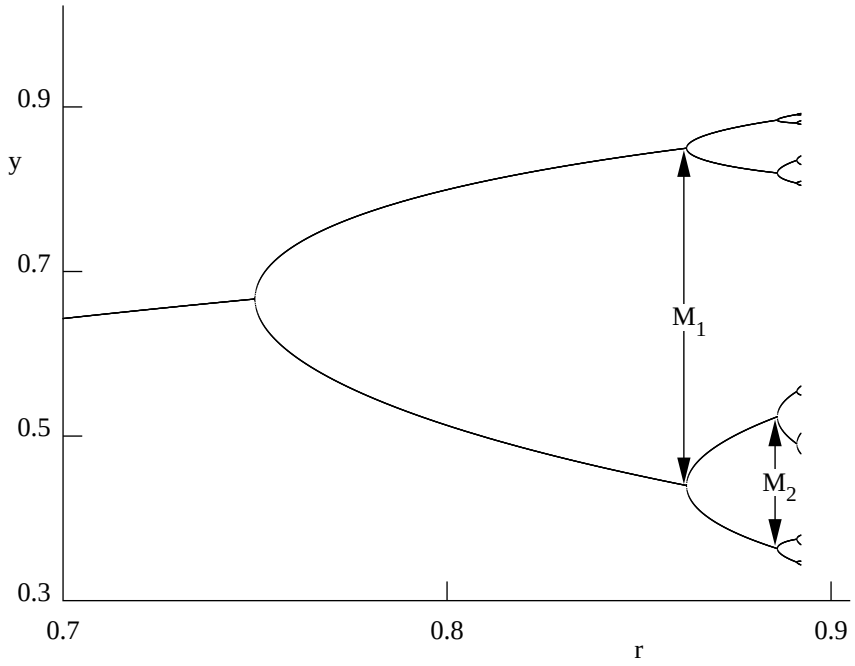

Figure 6.5: The first few bifurcations of the logistic equation showing the scaling of the maximum distance M_k between the asymptotic values of x describing the bifurcation.

The ratios $\alpha = (0.3090/0.1164) = 2.65$ for $k = 1$ and $\alpha = (0.1164/0.0460) = 2.53$ for $k = 2$ are consistent with the asymptotic value $\alpha = 2.5029078750958928485\ldots$

We now give qualitative arguments that suggest that the general behavior of the logistic map in the period doubling regime is independent of the detailed form of $f(x)$. As we have seen, period doubling is characterized by self-similarities, for example, the period doublings look similar except for a change of scale. We can demonstrate these similarities by comparing $f(x)$ for $r = s_1 = 0.5$ for the superstable trajectory with period 1 to the function $f^{(2)}(x)$ for $r = s_2 \approx 0.809017$ for the superstable trajectory of period 2 (see Figure 6.7). The function $f(x, r = s_1)$ has unstable fixed points at $x = 0$ and $x = 1$ and a stable fixed point at $x = 1/2$. Similarly the function $f^{(2)}(x, r = s_2)$ has a stable fixed point at $x = 1/2$ and an unstable fixed point at $x \approx 0.69098$. Note the similar shape, but different scale of the curves in the square boxes in part (a) and part (b) of Figure 6.7. This similarity is an example of scaling. That is, if we scale $f^{(2)}$ and change *(renormalize)* the value of r, we can compare $f^{(2)}$ to f. (See Chapter **??** for a discussion of scaling and renormalization in another context.)

This graphical comparison is meant only to be suggestive. A precise approach shows that if we continue the comparison of the higher-order iterates, for example, $f^{(4)}(x)$ to $f^{(2)}(x)$, etc., the superposition of functions converges to a universal function that is independent of the form of the original function $f(x)$.

Problem 6.9. Further determinations of the exponents α and δ

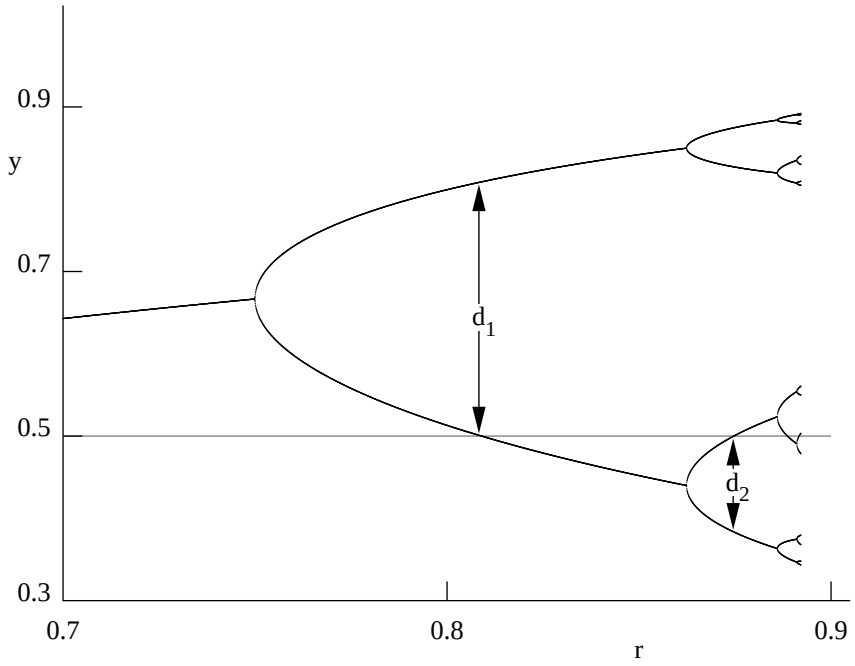

Figure 6.6: The quantity d_k is the distance from $x^* = 1/2$ to the nearest element of the attractor of period 2^k. It is convenient to use this quantity to determine the exponent α.

1. Determine the appropriate scaling factor and superimpose f and the rescaled form of $f^{(2)}$ found in Figure 6.7.

2. Use arguments similar to those discussed in the text and in Figure 6.7 and compare the behavior of $f^{(4)}(x, r = s_3)$ in the square about $x = 1/2$ with $f^{(2)}(x, r = s_2)$ in its square about $x = 1/2$. The size of the squares are determined by the unstable fixed point nearest to $x = 1/2$. Find the appropriate scaling factor and superimpose $f^{(2)}$ and the rescaled form of $f^{(4)}$. ■

*__Problem 6.10.__ Other one-dimensional maps

It is easy to modify your programs to consider other one-dimensional maps. Determine the qualitative properties of the one-dimensional maps:

$$f(x) = xe^{r(1-x)} \tag{6.13}$$

$$f(x) = r \sin \pi x. \tag{6.14}$$

Do they also exhibit the period doubling route to chaos? The map in (6.13) has been used by ecologists (cf. May) to study a population that is limited at high densities by the effect of epidemics. Although it is more complicated than (6.5), its advantage is that the population remains positive

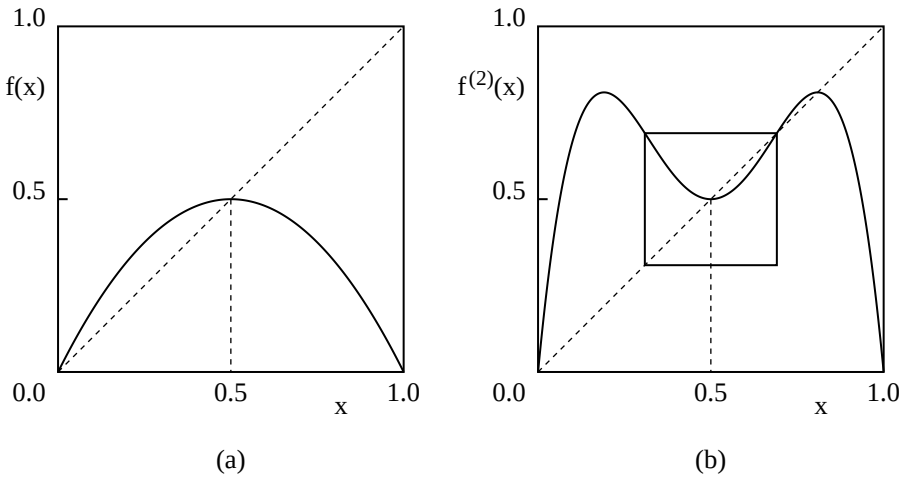

Figure 6.7: Comparison of $f(x,r)$ for $r = s_1$ with the second iterate $f^{(2)}(x)$ for $r = s_2$. (a) The function $f(x, r = s_1)$ has unstable fixed points at $x = 0$ and $x = 1$ and a stable fixed point at $x = 1/2$. (b) The function $f^{(2)}(x, r = s_1)$ has a stable fixed point at $x = 1/2$. The unstable fixed point of $f^{(2)}(x)$ nearest to $x = 1/2$ occurs at $x \approx 0.69098$, where the curve $f^{(2)}(x)$ intersects the line $y = x$. The upper right-hand corner of the square box in (b) is located at this point, and the center of the box is at $(1/2, 1/2)$. Note that if we reflect this square about the point $(1/2, 1/2)$, the shape of the reflected graph in the square box is nearly the same as it is in part (a), but on a smaller scale.

no matter what (positive) value is taken for the initial population. There are no restrictions on the maximum value of r, but if r becomes sufficiently large, x eventually becomes effectively zero. What is the behavior of the time series of (6.13) for $r = 1.5, 2$, and 2.7? Describe the qualitative behavior of $f(x)$. Does it have a maximum?

The sine map (6.14) with $0 < r \leq 1$ and $0 \leq x \leq 1$ has no special significance, except that it is nonlinear. If time permits, determine the approximate value of δ for both maps. What limits the accuracy of your determination of δ?

The above qualitative arguments and numerical results suggest that the quantities α and δ are *universal*, that is, independent of the detailed form of $f(x)$. In contrast, the values of the accumulation point r_∞ and the constant C in (6.9) depend on the detailed form of $f(x)$. Feigenbaum has shown that the period doubling route to chaos and the values of δ and α are universal properties of maps that have a quadratic maximum, that is, $f'(x)_{|x=x_m} = 0$ and $f''(x)_{|x=x_m} < 0$.

Why is the universality of period doubling and the numbers δ and α more than a curiosity? The reason is that because this behavior is independent of the details, there might exist realistic systems whose underlying dynamics yield the same behavior as the logistic map. Of course, most physical systems are described by differential rather than difference equations. Can these systems exhibit period doubling behavior? Several workers (cf. Testa et al.) have constructed nonlinear RLC circuits driven by an oscillatory source voltage. The output voltage shows bifurcations, and the measured values of the exponents δ and α are consistent with the predictions of the logistic

map.

Of more general interest is the nature of turbulence in fluid systems. Consider a stream of water flowing past several obstacles. We know that at low flow speeds, the water flows past obstacles in a regular and time-independent fashion, called *laminar* flow. As the flow speed is increased (as measured by a dimensionless parameter called the Reynolds number), some swirls develop, but the motion is still time-independent. As the flow speed is increased still further, the swirls break away and start moving downstream. The flow pattern as viewed from the bank becomes time-dependent. For still larger flow speeds, the flow pattern becomes very complex and looks random. We say that the flow pattern has made a transition from laminar flow to *turbulent* flow.

This qualitative description of the transition to chaos in fluid systems is superficially similar to the description of the logistic map. Can fluid systems be analyzed in terms of the simple models of the type we have discussed here? In a few instances such as turbulent convection in a heated saucepan, period doubling and other types of transitions to turbulence have been observed. The type of theory and analysis we have discussed has suggested new concepts and approaches, and the study of turbulent flow is a subject of much current interest.

6.5 Measuring Chaos

How do we know if a system is chaotic? The most important characteristic of chaos is *sensitivity to initial conditions*. In Problem 6.4 for example, we found that the trajectories starting from $x_0 = 0.5$ and $x_0 = 0.5001$ for $r = 0.91$ become very different after a small number of iterations. Because computers only store floating numbers to a certain number of digits, the implication of this result is that our numerical predictions of the trajectories of chaotic systems are restricted to small time intervals. That is, sensitivity to initial conditions implies that even though the logistic map is deterministic, our ability to make numerical predictions of its trajectory is limited.

How can we quantify this lack of predictably? In general, if we start two identical dynamical systems from slightly different initial conditions, we expect that the difference between the trajectories will increase as a function of n. In Figure 6.8 we show a plot of the difference $|\Delta x_n|$ versus n for the same conditions as in Problem 6.4a. We see that roughly speaking, $\ln|\Delta x_n|$ is a linearly increasing function of n. This result indicates that the separation between the trajectories grows exponentially if the system is chaotic. This divergence of the trajectories can be described by the *Lyapunov* exponent λ, which is defined by the relation:

$$|\Delta x_n| = |\Delta x_0|\, e^{\lambda n}, \tag{6.15}$$

where Δx_n is the difference between the trajectories at time n. If the Lyapunov exponent λ is positive, then nearby trajectories diverge exponentially. Chaotic behavior is characterized by the *exponential divergence of nearby trajectories*.

A naive way of measuring the Lyapunov exponent λ is to run the same dynamical system twice with slightly different initial conditions and measure the difference of the trajectories as a function of n. We used this method to generate Figure 6.8. Because the rate of separation of the trajectories might depend on the choice of x_0, a better method would be to compute the rate of

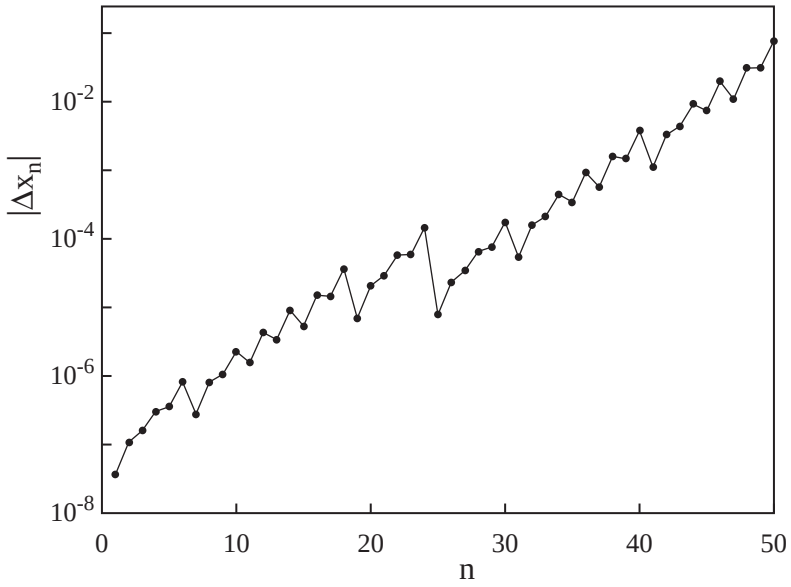

Figure 6.8: The evolution of the difference Δx_n between the trajectories of the logistic map at $r = 0.91$ for $x_0 = 0.5$ and $x_0 = 0.5001$. The separation between the two trajectories increases with n, the number of iterations, if n is not too large. (Note that $|\Delta x_1| \sim 10^{-8}$ and that the trend is not monotonic.)

separation for many values of x_0. This method would be tedious, because we would have to fit the separation to (6.15) for each value of x_0 and then determine an average value of λ.

A more important limitation of the naive method is that because the trajectory is restricted to the unit interval, the separation $|\Delta x_n|$ ceases to increase when n becomes sufficiently large. Fortunately, there is a better way of determining λ. We take the natural logarithm of both sides of (6.15), and write λ as

$$\lambda = \frac{1}{n} \ln \left| \frac{\Delta x_n}{\Delta x_0} \right|. \tag{6.16}$$

Because we want to use the data from the entire trajectory after the transient behavior has ended, we use the fact that

$$\frac{\Delta x_n}{\Delta x_0} = \frac{\Delta x_1}{\Delta x_0} \frac{\Delta x_2}{\Delta x_1} \cdots \frac{\Delta x_n}{\Delta x_{n-1}}. \tag{6.17}$$

Hence, we can express λ as

$$\lambda = \frac{1}{n} \sum_{i=0}^{n-1} \ln \left| \frac{\Delta x_{i+1}}{\Delta x_i} \right|. \tag{6.18}$$

The form (6.18) implies that we can interpret x_i for any i as the initial condition.

We see from (6.18) that the problem of computing λ has been reduced to finding the ratio $\Delta x_{i+1}/\Delta x_i$. Because we want to make the initial difference between the two trajectories as small as possible, we are interested in the limit $\Delta x_i \to 0$.

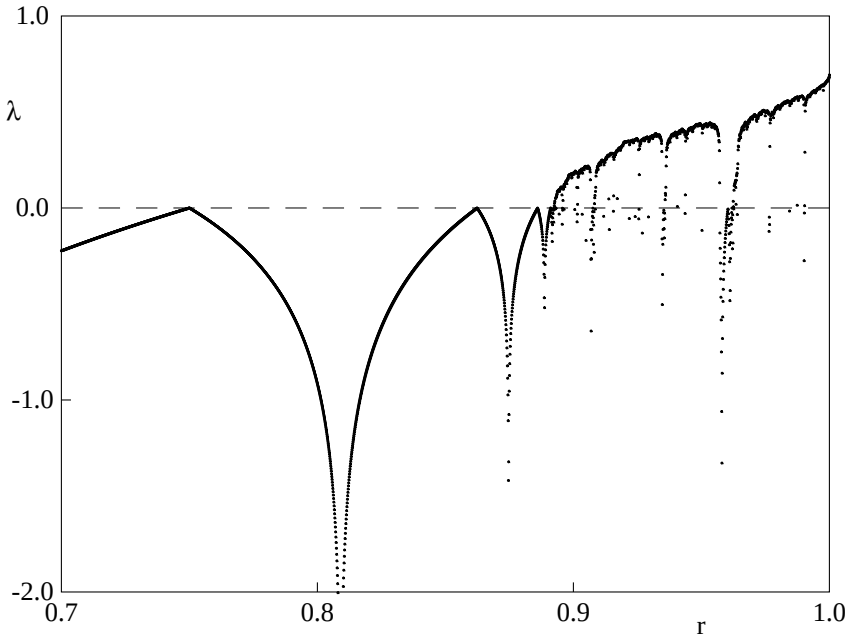

Figure 6.9: The Lyapunov exponent calculated using the method in (6.20) as a function of the control parameter r. Compare the behavior of λ to the bifurcation diagram in Figure 6.2. Note that $\lambda < 0$ for $r < 3/4$ and approaches zero at a period doubling bifurcation. A negative spike corresponds to a superstable trajectory. The onset of chaos is visible near $r = 0.892$, where λ first becomes positive. For $r \gtrsim 0.892$, λ generally increases except for dips below zero whenever a periodic window occurs, for example, the dip due to the period 3 window near $r = 0.96$. For each value of r, the first 1000 iterations were discarded, and 10^5 values of $\ln|f'(x_n)|$ were used to determine λ.

The idea of the more sophisticated procedure is to compute dx_{i+1}/dx_i from the equation of motion at the same time that the equation of motion is being iterated. We use the logistic map as an example. From (6.5) we have

$$\frac{dx_{i+1}}{dx_i} = f'(x_i) = 4r(1 - 2x_i). \tag{6.19}$$

We can consider x_i for any i as the initial condition and the ratio dx_{i+1}/dx_i as a measure of the rate of change of x_i. Hence, we can iterate the logistic map as before and use the values of x_i and the relation (6.19) to compute $f'(x_i) = dx_{i+1}/dx_i$ at each iteration. The Lyapunov exponent is given by

$$\lambda = \lim_{n\to\infty} \frac{1}{n} \sum_{i=0}^{n-1} \ln|f'(x_i)|\,, \tag{6.20}$$

where we begin the sum in (6.20) after the transient behavior is finished. We have included explicitly the limit $n \to \infty$ in (6.20) to remind ourselves to choose n sufficiently large. Note that

this procedure weights the points on the attractor correctly, that is, if a particular region of the attractor is not visited often by the trajectory, it does not contribute much to the sum in (6.20).

Exercise 6.11. Nearby trajectories

Create model to reproduce Figure 6.8 and compute the Lyapunov exponent λ using the naive approach. Choose $r = 0.91$, $x_0 = 0.5$, and $\Delta x_0 = 10^{-6}$, and plot $\ln|\Delta x_n/\Delta x_0|$ versus n. What happens to $\ln|\Delta x_n/\Delta x_0|$ for large n? Determine λ for $r = 0.91$, $r = 0.97$, and $r = 1.0$. Does your result for λ for each value of r depend significantly on your choice of x_0 or Δx_0?

Problem 6.12. Lyapunov exponent for the logistic map

a. Use the Logistic Lyapunov model to study λ using the algorithm discussed in the text for $r = 0.76$ to $r = 1.0$ in steps of $\Delta r = 0.01$. What is the sign of λ if the system is not chaotic? Plot λ versus r, and explain your results in terms of behavior of the bifurcation diagram shown in Figure 6.2. Compare your results for λ with those shown in Figure 6.9. How does the sign of λ correlate with the behavior of the system as seen in the bifurcation diagram? For what value of r is λ a maximum?

b. In Problem 6.4b we saw that roundoff errors in the chaotic regime make the computation of individual trajectories meaningless. That is, if the system's behavior is chaotic, then small roundoff errors are amplified exponentially in time, and the actual numbers we compute for the trajectory starting from a given initial value are not "real." Repeat your calculation of λ for $r = 1$ by changing the roundoff error as you did in Problem 6.4b. Does your computed value of λ change? How meaningful is your computation of the Lyapunov exponent? We will encounter a similar question in Chapter 8 where we compute the trajectories of chaotic systems of many particles. We will find that although the "true" trajectories cannot be computed for long times, averages over the trajectories yield meaningful results. ■

We have found that nearby trajectories diverge if $\lambda > 0$. For $\lambda < 0$, the two trajectories converge and the system is not chaotic. What happens for $\lambda = 0$? In this case we will see that the trajectories diverge algebraically, that is, as a power of n. In some cases a dynamical system is at the "edge of chaos" where the Lyapunov exponent vanishes. Such systems are said to exhibit weak chaos to distinguish their behavior from the strongly chaotic behavior ($\lambda > 0$) that we have been discussing.

If we define $z \equiv |\Delta x_n|/|\Delta x_0|$, then z will satisfy the differential equation

$$\frac{dz}{dn} = \lambda z. \tag{6.21}$$

For weak chaos we do not find an exponential divergence, but instead a divergence that is algebraic and is given by

$$\frac{dz}{dn} = \lambda_q z^q, \tag{6.22}$$

where q is a parameter that needs to be determined. The solution to (6.22) is

$$z = [1 + (1 - q)\lambda_q n]^{1/(1-q)}, \tag{6.23}$$

which can be checked by substituting (6.23) into (6.22). In the limit $q \to 1$, we recover the usual exponential dependence.

We can determine the type of chaos using the crude approach of choosing a large number of initial values of x_0 and $x_0 + \Delta x_0$ and plotting the average of $\ln z$ versus n. If we do not obtain a straight line, then the system does not exhibit strong chaos. How can we check for the behavior shown in (6.23)? The easiest way is to plot the quantity

$$\frac{z^{1-q} - 1}{1 - q} \tag{6.24}$$

versus n, which will equal $n\lambda_q$ if (6.23) is applicable. We explore these ideas in the following problem.

*__Problem 6.13.__ Measuring weak chaos

a. Write a program that plots $\ln z$ if $q = 1$ or z_q if $q \neq 1$ as a function of n. Your program should have q, $|\Delta x_0|$, the number of seeds, and the number of iterations as input parameters. To compare with work by Añaños and Tsallis, use a variation of the logistic map given by

$$x_{n+1} = 1 - ax_n^2, \tag{6.25}$$

where $|x_n| \leq 1$ and $0 \leq a \leq 2$. The seeds x_0 should be equally spaced in the interval $|x_0| < 1$.

b. Consider strong chaos at $a = 2$. Choose $q = 1$, 50 iterations, at least 1000 values of x_0, and $|\Delta x_0| = 10^{-6}$. Do you obtain a straight line for $\ln z$ versus n? Does z_n eventually stop increasing as a function of n? If so why? Try $|\Delta x_0| = 10^{-12}$. How do your results differ and how are they the same? Also iterate Δx directly:

$$\Delta x_{n+1} = x_{n+1} - \tilde{x}_{n+1} = -a(x_n^2 - \tilde{x}_n^2) = -a(x_n - \tilde{x}_n)(x_n + \tilde{x}_n) = -a\Delta x_n(x_n + \tilde{x}_n), \tag{6.26}$$

where x_n is the iterate starting at x_0 and $\tilde{x}_n$ is the iterate starting at $x_0 + \Delta x_0$. Show that straight lines are not obtained for your plot if $q \neq 1$.

c. The edge of chaos for this map is at $a = 1.401155189$. Repeat part (a) for this value of a and various values of q. Simulations with 10^5 values of x_0 points show that linear behavior is obtained for $q \approx 0.36$.

A system of fixed energy (and number of particles and volume) has an equal probability of being in any microstate specified by the positions and velocities of the particles (see Sec **??**). One way of measuring the ability of a system to be in any state is to measure its entropy defined by

$$S = -\sum_i p_i \ln p_i, \tag{6.27}$$

where the sum is over all states and p_i is the probability or relative frequency of being in the ith state. For example, if the system is always in only one state, then $S = 0$, the smallest possible entropy. If the system explores all states equally, then $S = \ln \Omega$, where Ω is the number of possible states. (You can show this result by letting $p_i = 1/\Omega$.)

*__Problem 6.14.__ Entropy of the logistic map

a. Write a program to compute S for the logistic map. Divide the interval $[0,1]$ into bins or subintervals of width $\Delta x = 0.01$ and determine the relative number of times the trajectory falls into each bin. At each value of r in the range $0.7 \leq r \leq 1$. the map should be iterated for a fixed number of steps, for example, $n = 1000$. Choose $\Delta x = 0.01$. What happens to the entropy when the trajectory is chaotic?

b. Repeat part (a) with $n = 10000$. For what values of r does the entropy change significantly? Decrease Δx to 0.001 and repeat. Does this decrease make a difference?

c. Plot p_i as a function of x for $r = 1$. For what value(s) of x is the plot a maximum?

We also can measure the (generalized) entropy as a function of time. As we will see in Problem 6.15, $S(n)$ for strong chaos increases linearly with n until all the possible states are visited. However, for weak chaos this behavior is not found. In the latter case we can generalize the entropy to a q-dependent function defined by

$$S_q = \frac{1 - \sum_i p_i^q}{q - 1}. \tag{6.28}$$

In the limit $q \to 1$, $S_q \to S$. The following problem discusses measuring the entropy for the same system as in Problem 6.13.

*__Problem 6.15.__ Entropy of weak and strong chaotic systems

a. Write a program that iterates the map (6.25) and plots S if $q = 1$ or S_q if $q \neq 1$ as a function of n. The input parameters should be q, the number of bins, the number of random seeds in a single bin, and n, the number of iterations. At each iteration compute the entropy. Then average S over the randomly chosen values of the seeds.

b. Consider strong chaos at $a = 2$. Choose $q = 1$, $n = 20$, at $\Delta x \leq 0.001$, and ten times as randomly chosen seeds per bin. Do you obtain a straight line for S versus n? Does the curve eventually stop growing? If you decrease Δx, how do your results differ and how are they the same? Show that S is not a linear function of n if $q \neq 1$.

c. Repeat part (a) with $a = 1.401155189$ and various values of q. Simulations with 10^5 bins show that linear behavior is obtained for $q \approx 0.36$, the same value as for the measurements in Problem 6.13.

6.6 *Controlling Chaos

6.7 Higher-Dimensional Models

6.8 Forced Damped Pendulum

6.9 *Hamiltonian Chaos

6.10 Perspective

As the many books and review articles on chaos can attest, it is impossible to discuss all aspects of chaos in a single chapter. We will revisit chaotic systems in Chapter **??** where we introduce the concept of fractals. We will find that one of the characteristics of chaotic dynamics is that the resulting attractors often have an intricate geometrical structure.

The most general ideas that we have discussed in this chapter are that *simple systems can exhibit complex behavior* and that chaotic systems exhibit *extreme sensitivity to initial conditions*. We also have learned that computers allow us to explore the behavior of dynamical systems and visualize the numerical output. However, the simulation of a system does not automatically lead to understanding. If you are interested in learning more about the phenomena of chaos and the associated theory, the suggested readings at the end of the chapter are a good place to start. We also invite you to explore chaotic phenomenon in more detail in the following projects.

6.11 Projects

The first several projects are on various aspects of the logistic map. These projects do not exhaust the possible investigations of the properties of the logistic map.

Project 6.16. A more accurate determination of δ and α

We have seen that it is difficult to determine δ accurately by finding the sequence of values of b_k at which the trajectory bifurcates for the kth time. A better way to determine δ is to compute it from the sequence s_m of superstable trajectories of period 2^{m-1}. We already have found that $s_1 = 1/2$, $s_2 \approx 0.80902$, and $s_3 \approx 0.87464$. The parameters s_1, $s_2, \ldots$ can be computed directly from the equation

$$f^{(2^{m-1})}(x = \frac{1}{2}) = \frac{1}{2}. \tag{6.29}$$

For example, s_2 satisfies the relation $f^{(2)}(x = 1/2) = 1/2$. This relation, together with the analytical form for $f^{(2)}(x)$ given in (6.8), yields:

$$8r^2(1 - r) - 1 = 0. \tag{6.30}$$

If we wish to solve (6.30) numerically for $r = s_2$, we need to be careful not to find the irrelevant solutions corresponding to a lower period. In this case we can factor out the solution $r = 1/2$ and

m	period	s_m
1	1	0.500 000 000
2	2	0.809 016 994
3	4	0.874 640 425
4	8	0.888 660 970
5	16	0.891 666 899
6	32	0.892 310 883
7	64	0.892 448 823
8	128	0.892 478 091

Table 6.2: Values of the control parameter s_m for the superstable trajectories of period 2^{m-1}. Nine decimal places are shown.

solve the resultant quadratic equation analytically to find $s_2 = (1 + \sqrt{5})/4$. Clearly $r = s_1 = 1/2$ solves (6.30) with period 1, because from (6.29), $f^{(1)}(x = 1/2) = 4r\frac{1}{2}(1 - \frac{1}{2}) = r = 1/2$ only for $r = 1/2$.

1. It is straightforward to adapt the bisection method discussed in Section 6.6. Adapt the class `RecursiveFixedPointApp` to find the numerical solutions of (6.29). Good starting values for the left-most and right-most values of r are easy to obtain. The left-most value is $r = r_\infty \approx 0.8925$. If we already know the sequence $s_1, s_2, \ldots, s_m$, then we can determine δ by
$$\delta_m = \frac{s_{m-1} - s_{m-2}}{s_m - s_{m-1}}. \tag{6.31}$$
We use this determination for δ_m to find the right-most value of r:
$$r_{\text{right}}^{(m+1)} = \frac{s_m - s_{m-1}}{\delta_m}. \tag{6.32}$$
We choose the desired precision to be 10^{-16}. A summary of our results is given in Table 6.2. Verify these results and determine δ.

2. Use your values of s_m to obtain a more accurate determination of α and δ.

Project 6.17. From chaos to order

The bifurcation diagram of the logistic map (see Figure 6.2) has many interesting features that we have not explored. For example, you might have noticed that there are several smooth dark bands in the chaotic region for $r > r_\infty$. Use `BifurcateApp` to generate the bifurcation diagram for $r_\infty \le r \le 1$. If we start at $r = 1.0$ and decrease r, we see that there is a band that narrows and eventually splits into two parts at $r \approx 0.9196$. If you look closely, you will see that the band splits into four parts at $r \approx 0.899$. If you look even more closely, you will see many more bands. What type of change occurs near the splitting (merging) of these bands)? Use `IterateMap` to look at the time series of (6.5) for $r = 0.9175$. You will notice that although the trajectory looks random, it oscillates back and forth between two bands. This behavior can be seen more clearly if you look at the time series of $x_{n+1} = f^{(2)}(x_n)$. A detailed discussion of the splitting of the bands can be found in Peitgen et al.

Project 6.18. Calculation of the Lyapunov spectrum

In Section 6.12 we discussed the calculation of the Lyapunov exponent for the logistic map. If a dynamical system has a multidimensional phase space, for example, the Hénon map and the Lorenz model, there is a set of Lyapunov exponents, called the Lyapunov spectrum, that characterize the divergence of the trajectory. As an example, consider a set of initial conditions that forms a filled sphere in phase space for the (three-dimensional) Lorenz model. If we iterate the Lorenz equations, then the set of phase space points will deform into another shape. If the system has a fixed point, this shape contracts to a single point. If the system is chaotic, then, typically, the sphere will diverge in one direction, but become smaller in the other two directions. In this case we can define three Lyapunov exponents to measure the deformation in three mutually perpendicular directions. These three directions generally will not correspond to the axes of the original variables. Instead, we must use a Gram-Schmidt orthogonalization procedure.

The algorithm for finding the Lyapunov spectrum is as follows:

(i) Linearize the dynamical equations. If $\mathbf{r}$ is the f-component vector containing the dynamical variables, then define $\Delta\mathbf{r}$ as the linearized difference vector. For example, the linearized Lorenz equations are

$$\frac{d\Delta x}{dt} = -\sigma\Delta x + \sigma\Delta y \tag{6.33a}$$

$$\frac{d\Delta y}{dt} = -x\Delta z - z\Delta x + r\Delta x - \Delta y \tag{6.33b}$$

$$\frac{d\Delta z}{dt} = x\Delta y + y\Delta x - b\Delta z. \tag{6.33c}$$

(ii) Define f orthonormal initial values for $\Delta\mathbf{r}$. For example, $\Delta\mathbf{r}_1(0) = (1, 0, 0)$, $\Delta\mathbf{r}_2(0) = (0, 1, 0)$, and $\Delta\mathbf{r}_3(0) = (0, 0, 1)$. Because these vectors appear in a linearized equation, they do not have to be small in magnitude.

(iii) Iterate the original and linearized equations of motion. One iteration yields a new vector from the original equation of motion and f new vectors $\Delta\mathbf{r}_\alpha$ from the linearized equations.

(iv) Find the orthonormal vectors $\Delta\mathbf{r}'_\alpha$ from the $\Delta\mathbf{r}_\alpha$ using the Gram-Schmidt procedure. That is,

$$\Delta\mathbf{r}'_1 = \frac{\Delta\mathbf{r}_1}{|\Delta\mathbf{r}_1|} \tag{6.34a}$$

$$\Delta\mathbf{r}'_2 = \frac{\Delta\mathbf{r}_2 - (\Delta\mathbf{r}'_1 \cdot \Delta\mathbf{r}_2)\Delta\mathbf{r}'_1}{|\Delta\mathbf{r}_2 - (\Delta\mathbf{r}'_1 \cdot \Delta\mathbf{r}_2)\Delta\mathbf{r}'_1|} \tag{6.34b}$$

$$\Delta\mathbf{r}'_3 = \frac{\Delta\mathbf{r}_3 - (\Delta\mathbf{r}'_1 \cdot \Delta\mathbf{r}_3)\Delta\mathbf{r}'_1 - (\Delta\mathbf{r}'_2 \cdot \Delta\mathbf{r}_3)\Delta\mathbf{r}'_2}{\left|\Delta\mathbf{r}_3 - (\Delta\mathbf{r}'_1 \cdot \Delta\mathbf{r}_3)\Delta\mathbf{r}'_1 - (\Delta\mathbf{r}'_2 \cdot \Delta\mathbf{r}_3)\Delta\mathbf{r}'_2\right|}. \tag{6.34c}$$

It is straightforward to generalize the method to higher dimensional models.

(v) Set the $\Delta\mathbf{r}_\alpha(t)$ equal to the orthonormal vectors $\Delta\mathbf{r}'_\alpha(t)$.

(vi) Accumulate the running sum, S_α as $S_\alpha \to S_\alpha + \log|\Delta\mathbf{r}_\alpha(t)|$.

(vii) Repeat steps (iii)–(vi) and periodically output the approximate Lyapunov exponents $\lambda_\alpha = (1/n)S_\alpha$, where n is the number of iterations.

To obtain a result for the Lyapunov spectrum that represent the steady state attractor, only include data after the transient behavior has ended.

a. Compute the Lyapunov spectrum for the Lorenz model for $\sigma = 16$, $b = 4$, and $r = 45.92$. Try other values of the parameters and compare your results.

b. Linearize the equations for the Hénon map and find the Lyapunov spectrum for $a = 1.4$ and $b = 0.3$ in (**??**).

Project 6.19. A spinning magnet

Consider a compass needle that is free to rotate in a periodically reversing magnetic field which is perpendicular to the axis of the needle. The equation of motion of the needle is given by

$$\frac{d^2\phi}{dt^2} = -\frac{\mu}{I} B_0 \cos\omega t \sin\phi, \tag{6.35}$$

where ϕ is the angle of the needle with respect to a fixed axis along the field, μ is the magnetic moment of the needle, I its moment of inertia, and B_0 and ω are the amplitude and the angular frequency of the magnetic field, respectively. Choose an appropriate numerical method for solving (6.35), and plot the Poincaré map at time $t = 2\pi n/\omega$. Verify that if the parameter $\lambda = \sqrt{2B_0\mu/I/\omega^2} > 1$, then the motion of the needle exhibits chaotic motion. Briggs (see references) discusses how to construct the corresponding laboratory system and other nonlinear physical systems.

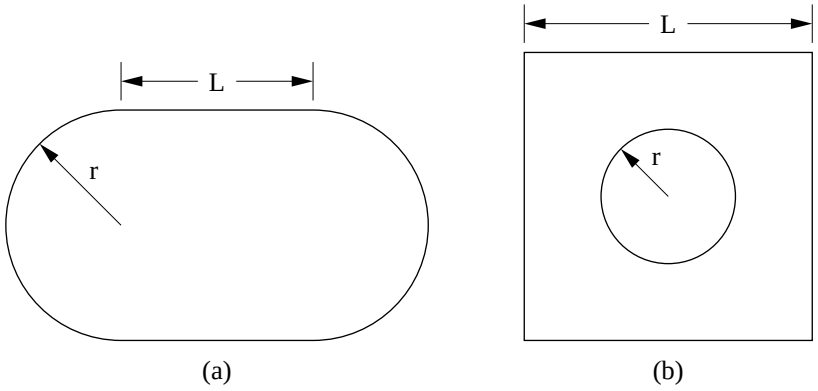

Figure 6.10: (a) Geometry of the stadium billiard model. (b) Geometry of the Sinai billiard model.

Project 6.20. Billiard models

Consider a two-dimensional planar geometry in which a particle moves with constant velocity along straight line orbits until it elastically reflects off the boundary. This straight line motion occurs in various "billiard" systems. A simple example of such a system is a particle moving with fixed speed

within a circle. For this geometry the angle between the particle's momentum and the tangent to the boundary at a reflection is the same for all points.

Suppose that we divide the circle into two equal parts and connect them by straight lines of length L as shown in Figure 6.10a. This geometry is called a *stadium billiard*. How does the motion of a particle in the stadium compare to the motion in the circle? In both cases we can find the trajectory of the particle by geometrical considerations. The stadium billiard model and a similar geometry known as the Sinai billiard model (see Figure 6.10b) have been used as model systems for exploring the foundations of statistical mechanics. There also is much interest in relating the behavior of a classical particle in various billiard models to the solution of Schrödinger's equation for the same geometries.

a. Write a program to simulate the stadium billiard model. Use the radius r of the semicircles as the unit of length. The algorithm for determining the path of the particle is as follows:

   (i) Begin with an initial position (x_0, y_0) and momentum (p_{x0}, p_{y0}) of the particle such that $|\mathbf{p}_0| = 1$.

   (ii) Determine which of the four sides the particle will hit. The possibilities are the top and bottom line segments and the right and left semicircles.

   (iii) Determine the next position of the particle from the intersection of the straight line defined by the current position and momentum, and the equation for the segment where the next reflection occurs.

   (iv) Determine the new momentum, (p'_x, p'_y), of the particle after reflection such that the angle of incidence equals the angle of reflection. For reflection off the line segments we have $(p'_x, p'_y) = (p_x, -p_y)$. For reflection off a circle we have

$$p'_x = \left[y^2 - (x - x_c)^2\right]p_x - 2(x - x_c)yp_y \tag{6.36a}$$

$$p'_y = -2(x - x_c)yp_x + \left[(x - x_c)^2 - y^2\right]p_y, \tag{6.36b}$$

   where $(x_c, 0)$ is the center of the circle. (Note that the momentum p_x rather than p'_x is on the right-hand side of (6.36b). Remember that all lengths are scaled by the radius of the circle.)

   (v) Repeat steps (ii)–(iv).

b. Determine if the particle dynamics is chaotic by estimating the largest Lyapunov exponent. One way to do so is to start two particles with almost identical positions and/or momenta (varying by say 10^{-5}). Compute the difference Δs of the two phase space trajectories as a function of the number of reflections n, where Δs is defined by

$$\Delta s = \sqrt{|\mathbf{r}_1 - \mathbf{r}_2|^2 + |\mathbf{p}_1 - \mathbf{p}_2|^2}. \tag{6.37}$$

   Choose $L = 1$ and $r = 1$. The Lyapunov exponent can be found from a semilog plot of Δs versus n. Repeat your calculation for different initial conditions and average your values of Δs before plotting. Repeat the calculation for $L = 0.5$ and 2.0 and determine if your results depend on L.

c. Another test for the existence of chaos is the reversibility of the motion. Reverse the momentum after the particle has made n reflections, and let the drawing color equal the background color so that the path can be erased. What limitation does roundoff error place on your results? Repeat this simulation for $L = 1$ and $L = 0$.

d. Place a small hole of diameter d in one of the circular sections of the stadium so that the particle can escape. Choose $L = 1$ and set $d = 0.02$. Give the particle a random position and momentum, and record the time when the particle escapes through the hole. Repeat for at least 10^4 particles and compute the fraction of particles $S(n)$ remaining after a given number of reflections n. The function $S(n)$ will decay with n. Determine the functional dependence of S on n, and calculate the characteristic decay time if $S(n)$ decays exponentially. Repeat for $L = 0.1$, 0.5, and 2.0. Is the decay time a function of L? Does $S(n)$ decays exponentially for the circular billiard model ($L = 0$) (see Bauer and Bertsch)?

e. Choose an arbitrary initial position for the particle in a stadium with $L = 1$, and a small hole as in part (d). Choose at least 5000 values of the initial value p_{x0} uniformly distributed between 0 and 1. Choose p_{y0} so that $|\mathbf{p}| = 1$. Plot the escape time versus p_{x0}, and describe the visual pattern of the trajectories. Then choose 5000 values of p_{x0} in a smaller interval centered about the value of p_{x0} for which the escape time was greatest. Plot these values of the escape time versus p_{x0}. Do you see any evidence of self-similarity?

f. Repeat steps (a)–(e) for the Sinai billiard geometry.

Project 6.21. The circle map and mode locking

The driven, damped pendulum can be approximated by a one-dimensional difference equation for a range of amplitudes and frequencies of the driving force. This difference equation is known as the *circle map* and is given by

$$\theta_{n+1} = \left(\theta_n + \Omega - \frac{K}{2\pi}\sin 2\pi\theta_n\right). \quad \text{(modulo 1)} \tag{6.38}$$

The variable θ represents an angle, and Ω represents a frequency ratio, the ratio of the natural frequency of the pendulum to the frequency of the periodic driving force. The parameter K is a measure of the strength of the nonlinear coupling of the pendulum to the external force. An important quantity is the winding number which is defined as

$$W = \lim_{m\to\infty} \frac{1}{m}\sum_{n=0}^{m-1} \Delta\theta_n, \tag{6.39}$$

where $\Delta\theta_n = \Omega - (K/2\pi)\sin 2\pi\theta_n$.

a. Consider the linear case, $K = 0$. Choose $\Omega = 0.4$ and $\theta_0 = 0.2$ and determine W. Verify that if Ω is a ratio of two integers, then $W = \Omega$ and the trajectory is periodic. What is the value of W if $\Omega = \sqrt{2}/2$, an irrational number? Verify that $W = \Omega$ and that the trajectory comes arbitrarily close to any particular value of θ. Does θ_n ever return exactly to its initial value? This type of behavior of the trajectory is termed *quasiperiodic*.

b. For $K > 0$, we will find that $W \neq \Omega$ and "locks" into rational frequency ratios for a range of values of K and Ω. This type of behavior is called *mode locking*. For $K < 1$, the trajectory is either periodic or quasiperiodic. Determine the value of W for $K = 1/2$ and values of Ω in the range $O < \Omega \leq 1$. The widths in Ω of the various mode-locked regions where W is fixed increase with K. Consider other values of K, and draw a diagram in the K-Ω plane ($0 \leq K, \Omega \leq 1$) so that those areas corresponding to frequency locking are shaded. These shaded regions are called *Arnold tongues*.

c. For $K = 1$, all trajectories are frequency-locked periodic trajectories. Fix K at $K = 1$ and determine the dependence of W on Ω. The plot of W versus Ω for $K = 1$ is called the *Devil's staircase*.

Project 6.22. Chaotic scattering

In Chapter 5 we discussed the classical scattering of particles off a fixed target, and found that the differential cross section for a variety of interactions is a smoothly varying function of the scattering angle. That is, a small change in the impact parameter b leads to a small change in the scattering angle θ. Here we consider examples where a small change in b leads to large changes in θ. Such a phenomenon is called *chaotic scattering*, because of the sensitivity to initial conditions that is characteristic of chaos. The study of chaotic scattering is relevant to the design of electronic nanostructures, because many experimental structures exhibit this type of scattering.

A typical scattering model consists of a target composed of a group of fixed hard disks and a scatterer consisting of a point particle. The goal is to compute the path of the scatterer as it bounces off the disks, and measure θ and the time of flight as a function of the impact parameter b. If a particle bounces inside the target region before leaving, the time of flight can be very long. There are even some trajectories for which the particle never leaves the target region.

Because it is difficult to monitor a trajectory that bounces back and forth between the hard disks, we instead consider a two-dimensional map that contains the key features of chaotic scattering (see Yalcinkaya and Lai for further discussion). The map is given by

$$x_{n+1} = a\big[x_n - \frac{1}{4}(x_n + y_n)^2\big], \tag{6.40a}$$

$$y_{n+1} = \frac{1}{a}\big[y_n + \frac{1}{4}(x_n + y_n)^2\big], \tag{6.40b}$$

where a is a parameter. The target region is centered at the origin. In an actual scattering experiment, the relation between (x_{n+1}, y_{n+1}) and (x_n, y_n) would be much more complicated, but the map (6.40) captures most of the important features of realistic chaotic scattering experiments. The iteration number n is analogous to the number of collisions of the scattered particle off the disks. When x_n or y_n is significantly different from zero, the scatterer has left the target region.

a. Write a program to iterate the map (6.40). Let $a = 8.0$ and $y_0 = -0.3$. Choose 10^4 initial values of x_0 uniformly distributed in the interval $0 < x_0 < 0.1$. Determine the time $T(x_0)$, the number of iterations for which $x_n \leq -5.0$. After this time, x_n rapidly moves to $-\infty$. Plot $T(x_0)$ versus x_0. Then choose 10^4 initial values in a smaller interval centered about a value of x_0 for which $T(x_0) > 7$. Plot these values of $T(x_0)$ versus x_0. Do you see any evidence of self-similarity?

b. A trajectory is said to be *uncertain* if a small change ϵ in x_0 leads to a change in $T(x_0)$. We expect that the number of uncertain trajectories, N, will depend on a power of ϵ, that is, $N \sim \epsilon^{\alpha}$. Determine $N(\epsilon)$ for $\epsilon = 10^{-p}$ with $p = 2$ to 7 using the values of x_0 in part (a). Then determine the uncertainty dimension $1 - \alpha$ from a log-log plot of N versus ϵ. Repeat these measurements for other values of a. Does α depend on a?

c. Choose 4×10^4 initial conditions in the same interval as in part (a) and determine the number of trajectories, $S(n)$, that have not yet reached $x_n = -5$ as a function of the number of iterations n. Plot $\ln S(n)$ versus n and determine if the decay is exponential. It is possible to obtain algebraic decay for values of a less than approximately 6.5.

d. Let $a = 4.1$ and choose 100 initial conditions uniformly distributed in the region $1.0 < x_0 < 1.05$ and $0.60 < y_0 < 0.65$. Are there any trajectories that are periodic and hence have infinite escape times? Due to the accumulation of roundoff error, it is possible to find only finite, but very long escape times. These periodic trajectories form closed curves, and the regions enclosed by them are called KAM surfaces.

Project 6.23. Chemical reactions

In Project 4.20 we discussed how chemical oscillations can occur when the reactants are continuously replenished. In this project we introduce a set of chemical reactions that exhibits the period doubling route to chaos. Consider the following reactions (see Peng et al.):

$$P \to A \tag{6.41a}$$
$$P + C \to A + C \tag{6.41b}$$
$$A \to B \tag{6.41c}$$
$$A + 2B \to 3B \tag{6.41d}$$
$$B \to C \tag{6.41e}$$
$$C \to D. \tag{6.41f}$$

Each of the above reactions has an associated rate constant. The time dependence of the concentrations of A, B, and C is given by:

$$\frac{dA}{dt} = k_1 P + k_2 PC - k_3 A - k_4 AB^2 \tag{6.42a}$$
$$\frac{dB}{dt} = k_3 A + k_4 AB^2 - k_5 B \tag{6.42b}$$
$$\frac{dC}{dt} = k_4 B - k_5 C. \tag{6.42c}$$

We assume that P is held constant by replenishment from an external source. We also assume the chemicals are well mixed so that there is no spatial dependence. In Section **??** we discuss the effects of spatial inhomogeneities due to molecular diffusion. Equations (6.41) can be written in a

dimensionless form as

$$\frac{dX}{d\tau} = c_1 + c_2 Z - X - XY^2 \tag{6.43a}$$

$$c_3 \frac{dY}{d\tau} = X + XY^2 - Y \tag{6.43b}$$

$$c_4 \frac{dZ}{d\tau} = Y - Z, \tag{6.43c}$$

where the c_i are constants, $\tau = k_3 t$, and X, Y, and Z are proportional to A, B, and C, respectively.

a. Write a program to solve the coupled differential equations in (6.43). Use a fourth-order Runge-Kutta algorithm with an adaptive step size. Plot $\ln Y$ versus the time τ.

b. Set $c_1 = 10$, $c_3 = 0.005$, and $c_4 = 0.02$. The constant c_2 is the control parameter. Consider $c_2 = 0.10$ to 0.16 in steps of 0.005. What is the period of $\ln Y$ for each value of c_2?

c. Determine the values of c_2 at which the period doublings occur for as many period doublings as you can determine. Compute the constant δ (see (6.10)) and compare its value to the value of δ for the logistic map.

d. Make a bifurcation diagram by taking the values of $\ln Y$ from the Poincaré plot at $X = Z$ and plotting them versus the control parameter c_2. Do you see a sequence of period doublings?

e. Use three-dimensional graphics to plot the trajectory of (6.43) with $\ln X$, $\ln Y$, and $\ln Z$ as the three axes. Describe the attractors for some of the cases considered in part (a).

6.12 Simulations

The following models are implemented in *EJS* and are downloadable from the *OSP* Collection in the ComPADRE digital library. Additional simulations will be written for missing sections.

Iteration

The Iteration model computes a table of iterates $x_0, x_1, x_2, x_3, \cdots$ using a map $x_{n+1} = f(x_n)$ that computes a sequence of numbers starting with a seed x_0 and a control parameter r and repeatedly applying the map. The sequence of iterates is referred to as a trajectory or an orbit. See Section 6.2.

Logistic Bifurcation

The Bifurcation model shows the long-term iterates of the logistic map $x_{n+1} = 4rx_n(x_n - 1)$ as a function of the control parameter r. The model plots the iterated values x_n after the initial transient behavior is discarded. If the trajectory is close to an attractor, only those points that lie on the attractor will appear on the plot. The Bifurcation model nicely shows the forking of the possible periods of stable orbits from 1 to 2 to 4 to 8 etc. as r is increased. Each of these bifurcation points is a period-doubling bifurcation. See Section 6.2.

Logistic Cobweb

The Logistic Cobweb model shows the behavior of the logistic map by showing a cobweb plot, a table of iterates, and a plot of iterates. The cobweb plot consists of a diagonal ($x = y$) line and a curve representing $y = 4rx(1 - x)$. Starting with an initial seed x_0, the plot shows how visually how the logistic map produces successive iterates. The cobweb spirals inward toward a stable fixed point. Period doubling produces closed loops, and chaotic orbits show a filled area. See Section .

Logistic Lyapunov

The Logistic Lyapunov Exponent model plots the Lyapunov exponent to shows the rate of separation of logistic map trajectories. See Section .

Two Ball Bounce

The Two Ball Bounce model shows a two-ball collision in a constant gravitational field that is constrained to move in one dimension above a fixed floor. Except when a collision occurs, each ball is a freely falling particle. The model also displays a Poincaré map using the velocity v_1 and height y_1 of the upper ball m1 at the instant that the lower ball m_2 hits the floor.

Appendix 6A: Stability of the Fixed Points of the Logistic Map

In the following, we derive analytical expressions for the fixed points of the logistic map. The fixed-point condition is given by

$$x^* = f(x^*). \tag{6.44}$$

From (6.5) this condition yields the two fixed points

$$x^* = 0 \quad \text{and} \quad x^* = 1 - \frac{1}{4r}. \tag{6.45}$$

Because x is restricted to be positive, the only fixed point for $r < 1/4$ is $x = 0$. To determine the stability of x^*, we let

$$x_n = x^* + \epsilon_n, \tag{6.46a}$$

and

$$x_{n+1} = x^* + \epsilon_{n+1}. \tag{6.46b}$$

Because $|\epsilon_n| \ll 1$, we have

$$x_{n+1} = f(x^* + \epsilon_n) \approx f(x^*) + \epsilon_n f'(x^*) = x^* + \epsilon_n f'(x^*). \tag{6.47}$$

If we compare (6.46b) and (6.47), we obtain

$$\epsilon_{n+1}/\epsilon_n = f'(x^*). \tag{6.48}$$

If $|f'(x^*)| > 1$, the trajectory will diverge from x^* because $|\epsilon_{n+1}| > |\epsilon_n|$. The opposite is true for $|f'(x^*)| < 1$. Hence, the local stability criteria for a fixed point x^* are

1. $|f'(x^*)| < 1$, x^* is stable;
2. $|f'(x^*)| = 1$, x^* is marginally stable;
3. $|f'(x^*)| > 1$, x^* is unstable.

If x^* is marginally stable, the second derivative $f''(x)$ must be considered, and the trajectory approaches x^* with deviations from x^* inversely proportional to the square root of the number of iterations.

For the logistic map the derivatives at the fixed points are respectively

$$f'(x=0) = \frac{d}{dx}[4rx(1-x)]\Big|_{x=0} = 4r, \tag{6.49}$$

and

$$f'(x=x^*) = \frac{d}{dx}[4rx(1-x)]\Big|_{x=1-1/4r} = 2-4r. \tag{6.50}$$

It is straightforward to use (6.49) and (6.50) to find the range of r for which $x^* = 0$ and $x^* = 1-1/4r$ are stable.

If a trajectory has period two, then $f^{(2)}(x) = f(f(x))$ has two fixed points. If you are interested, you can solve for these fixed points analytically. As we found in Problem 6.3, these two fixed points become unstable at the same value of r. We can derive this property of the fixed points using the chain rule of differentiation:

$$\frac{d}{dx}f^{(2)}(x)\big|_{x=x_0} = \frac{d}{dx}f(f(x))\big|_{x=x_0} = f'(f(x_0))f'(x)\big|_{x=x_0}. \tag{6.51}$$

If we substitute $x_1 = f(x_0)$, we can write

$$\frac{d}{dx}f(f(x))\big|_{x=x_0} = f'(x_1)f'(x_0). \tag{6.52}$$

In the same way, we can show that

$$\frac{d}{dx}f^{(2)}(x)\big|_{x=x_1} = f'(x_0)f'(x_1). \tag{6.53}$$

We see that if x_0 becomes unstable, then $|f^{(2)'}(x_0)| > 1$ as does $|f^{(2)'}(x_1)|$. Hence, x_1 also is unstable at the same value of r, and we conclude that both fixed points of $f^{(2)}(x)$ bifurcate at the same value of r, leading to an trajectory of period 4.

From (6.50) we see that $f'(x=x^*) = 0$ when $r = 1/2$ and $x^* = 1/2$. Such a fixed point is said to be superstable, because as we found in Problem 6.6, convergence to the fixed point is relatively rapid. Superstable trajectories occur whenever one of the fixed points is at $x^* = 1/2$.

Appendix 6B: Finding the Roots of a Function

The roots of a function $f(x)$ are the values of the variable x for which the function $f(x)$ is zero. Even an apparently simple equation such as

$$f(x) = \tan x - x - c = 0. \tag{6.54}$$

where c is a constant cannot be solved analytically for x.

Regardless of the function and the approach to root finding, the first step should be to learn as much as possible about the function. For example, plotting the function will help us to determine the approximate locations of the roots.

Newton's (or the Newton-Raphson) method is based on replacing the function by the first two terms of the Taylor expansion of $f(x)$ about the root x. If our initial guess for the root is x_0, we can write $f(x) \approx f(x_0) + (x - x_0)f'(x_0)$. If we set $f(x)$ equal to zero and solve for x, we find $x = x_0 - f(x_0)/f'(x_0)$. If we have made a good choice for x_0, the resultant value of x should be closer than x_0 to the root. The general procedure is to calculate successive approximations as follows:

$$x_{n+1} = x_n - \frac{f(x_n)}{f'(x_n)}. \tag{6.55}$$

If this series converges, it converges very quickly. However, if the initial guess is poor or if the function has closely spaced multiple roots, the series may not converge. The successive iterations of Newton's method is an another example of a map. Newton's method also works with complex functions as we will see in the following problem.

Problem 6.24. Cube roots

Consider the function $f(z) = z^3 - 1$, where $z = x + iy$, and $f'(z) = z^2$. Map the range of convergence of (6.55) in the region $[-2 < x < 2, -2 < y < 2]$ in the complex plane. Color the starting z value red, green, or blue depending on the root to which the initial guess converges. If the trajectory does not converge, color the starting point black. For more insight add a mouse handler to your program so that if you click on your plot, the sequence of iterations starting from the point where you clicked will be shown.

The following problem discusses a situation that typically arises in courses on quantum mechanics.

Problem 6.25. Energy levels in a finite square well

The quantum mechanical energy levels in the one-dimensional finite square well can be found by solving the relation:

$$\epsilon \tan \epsilon = \sqrt{\rho^2 - \epsilon^2}, \tag{6.56}$$

where $\epsilon = \sqrt{mEa^2/2\hbar}$ and $\rho = \sqrt{mV_0a^2/2\hbar}$ are defined in terms of the particle mass m, the particle energy E, the width of the well a, and the depth of the well V_0. The function $\epsilon \tan \epsilon$ has zeros at $\epsilon = 0, \pi, 2\pi, \ldots$ and asymptotes at $\epsilon = 0, \pi/2, 3\pi/2, 5\pi/2 \ldots$. The function $\sqrt{\rho - \epsilon^2}$ is a quarter circle of radius ρ. Write a program to plot these two functions with $\rho = 3$ and then use Newton's method to determine the roots of (6.56). Find the value of ρ and thus V_0, such that below this value there is only one energy level and above this value there is more than one. At what value of ρ do three energy levels first appear?

In Section 6.6 we introduced the bisection root finding algorithm. This algorithm is implemented in the `Root` class in the numerics package. It can be used with any function.

Listing 6.2: The `bisection` method defined in the `Root` class in the numerics package.

```
public static double bisection(final Function f, double x1, double x2, final double tol) {
  int count = 0;
  int maxCount = (int) (Math.log(Math.abs(x2 - x1) / tol) / Math.log(2));
  maxCount = Math.max(MAX_ITERATIONS, maxCount) + 2;
  double y1 = f.evaluate(x1), y2 = f.evaluate(x2);
  if (y1 * y2 > 0) { // y1 and y2 must have opposite sign
    return Double.NaN; // interval does not contain a root
  }
  while (count < maxCount) {
    double x = (x1 + x2) / 2;
    double y = f.evaluate(x);
    if (Math.abs(y) < tol)return x;
    if (y * y1 > 0) { // replace the end-point that has the same sign
      x1 = x;
      y1 = y;
    }
    else {
      x2 = x;
      y2 = y;
    }
    count++;
  }
  return Double.NaN; // did not converge in max iterations
}
```

The bisection algorithm is guaranteed to converge if you can find an interval where the function changes sign. However, it is slow. Newton's algorithm is very fast, but may not converge. We develop an algorithm in the following problem that combines these two approaches.

Problem 6.26. Finding roots

Modify Newton's algorithm to keep track of the interval between the minimum and the maximum of x while iterating (6.55). If the iterate x_{n+1} jumps outside this interval, interrupt Newton's method and use the bisection algorithm for one iteration. Test the root at the end of the iterative process to check that the algorithm actually found a root. Test your algorithm on the function in (6.54).

References and Suggestions for Further Reading

Books

Ralph H. Abraham and Christopher D. Shaw, *Dynamics – The Geometry of Behavior*, second edition, Addison-Wesley (1992). The authors use an abundance of visual representations.

Hao Bai-Lin, *Chaos II*, World Scientific (1990). A collection of reprints on chaotic phenomena. The following papers were cited in the text. James P. Crutchfield, J. Doyne Farmer, Norman H. Packhard, and Robert S. Shaw, "Chaos," Sci. Am. **255** (6), 46–57 (1986); Mitchell J. Feigenbaum, "Quantitative universality for a class of nonlinear transformations," J. Stat. Phys. **19**, 25–52 (1978); M. Hénon, "A two-dimensional mapping with a strange attractor," Commun. Math. Phys. **50**, 69–77 (1976); Robert M. May, "Simple mathematical models with very complicated dynamics," Nature **261**, 459–467 (1976); Robert Van Buskirk and Carson Jeffries, "Observation of chaotic dynamics of coupled nonlinear oscillators," Phys. Rev. A **31**, 3332–3357 (1985).

G. L. Baker and J. P. Gollub, *Chaotic Dynamics: An Introduction*, second edition, Cambridge University Press (1995). A good introduction to chaos with special emphasis on the forced damped nonlinear harmonic oscillator. Several programs are given.

Pedrag Cvitanovic, *Universality in Chaos*, second edition, Adam-Hilger (1989). A collection of reprints on chaotic phenomena including the articles by Hénon and May also reprinted in the Bai-Lin collection and the chaos classic, Mitchell J. Feigenbaum, "Universal behavior in nonlinear systems," Los Alamos Sci. **1**, 4–27 (1980).

Robert Devaney, *A First Course in Chaotic Dynamical Systems*, Addison-Wesley (1992). This text is a good introduction to the more mathematical ideas behind chaos and related topics.

Jan Fröyland, *Introduction to Chaos and Coherence*, Institute of Physics Publishing (1992). See Chapter 7 for a simple model of Saturn's rings.

Martin C. Gutzwiller, *Chaos in Classical and Quantum Mechanics*, Springer-Verlag (1990). A good introduction to problems in quantum chaos for the more advanced student.

Robert C. Hilborn, *Chaos and Nonlinear Dynamics*, Oxford University Press (1994). An excellent pedagogically oriented text.

Douglas R. Hofstadter, *Metamagical Themas*, Basic Books (1985). A shorter version is given in his article, "Metamagical themas," Sci. Am. **245** (11), 22–43 (1981).

E. Atlee Jackson, *Perspectives of Nonlinear Dynamics*, Vols. 1 and 2., Cambridge University Press (1989, 1991). An advanced text that is a joy to read.

R. V. Jensen, "Chaotic scattering, unstable periodic orbits, and fluctuations in quantum transport," Chaos **1**, 101–109 (1991). This paper discusses the quantum version of systems similar to those discussed in Projects 6.22 and 6.20.

Francis C. Moon, *Chaotic and Fractal Dynamics, An Introduction for Applied Scientists and Engineers*, Wiley (1992). An engineering oriented text with a section on how to build devices that demonstrate chaotic dynamics.

Edward Ott, *Chaos in Dynamical Systems*, Cambridge University Press (1993). An excellent textbook on chaos at the upper undergraduate to graduate level. See also E. Ott, "Strange attractors and chaotic motions of dynamical systems," Rev. Mod. Phys. **53**, 655–671 (1981).

Edward Ott, Tim Sauer, and James A. Yorke, editors, *Coping with Chaos*, John Wiley & Sons (1994). A reprint volume emphasizing the analysis of experimental time series from chaotic systems.

Heinz-Otto Peitgen, Hartmut Jürgens, and Dietmar Saupe, *Fractals for the Classroom*, Part II, Springer-Verlag (1992). A delightful book with many beautiful illustrations. Chapter 11 discusses the nature of the bifurcation diagram of the logistic map.

Ian Percival and Derek Richards, *Introduction to Dynamics*, Cambridge University Press (1982). An advanced undergraduate text that introduces phase trajectories and the theory of stability. A derivation of the Hamiltonian for the driven damped pendulum considered in Section 6.4 is given in Chapter 5, example 5.7.

Ivars Peterson, *Newton's Clock: Chaos in the Solar System*, W. H. Freeman (1993). An historical survey of our understanding of the motion of bodies within the solar system with a focus on chaotic motion.

Stuart L. Pimm, *The Balance of Nature*, The University of Chicago Press (1991). An introductory treatment of ecology with a chapter on applications of chaos to real biological systems. The author contends that much of the difficulty in assessing the importance of chaos is that ecological studies are too short.

William H. Press, Saul A. Teukolsky, William T. Vetterling, and Brian P. Flannery, *Numerical Recipes*, second edition, Cambridge University Press (1992). Chapter 9 discusses various root finding methods.

S. Neil Rasband, *Chaotic Dynamics of Nonlinear Systems*, Wiley-Interscience (1990). Clear presentation of the most important topics in classical chaos theory.

M. Lakshmanan and S. Rajaseekar, *Nonlinear Dynamics*, Springer-Verlag (2003). Although this text is for advanced students, many parts are accessible.

Robert Shaw, *The Dripping Faucet as a Model Chaotic System*, Aerial Press, Santa Cruz, CA (1984).

Steven Strogatz, *Nonlinear Dynamics and Chaos with Applications to Physics, Biology, Chemistry and Engineering*, Addison-Wesley (1994). Another outstanding text.

Anastasios A. Tsonis, *Chaos: From Theory to Applications*, Plenum Press (1992). Of particular interest is the discussion of applications nonlinear time series forecasting.

Nicholas B. Tufillaro, Tyler Abbott, and Jeremiah Reilly, *Nonlinear Dynamics and Chaos*, Addison-Wesley (1992) and at `<http://www.drchaos.net/drchaos/Book/node2.html>`. See also, N. B. Tufillaro and A. M. Albano, "Chaotic dynamics of a bouncing ball," Am. J. Phys. **54**, 939–944 (1986). The authors describe an undergraduate level experiment on a bouncing ball subject to repeated impacts with a vibrating table. See also the article by Warr et al.

Articles

Garin F. J. Añaños and Constantino Tsallis, "Ensemble averages and nonextensivity of one-dimensional maps, Phys. Rev. Lett. **93**, 020601 (2004).

Gregory L. Baker, "Control of the chaotic driven pendulum," Am. J. Phys. **63** (9), 832–838 (1995).

W. Bauer and G. F. Bertsch, "Decay of ordered and chaotic systems," Phys. Rev. Lett. **65**, 2213 (1990). See also the comment by Olivier Legrand and Didier Sornette, "First return, transient chaos, and decay in chaotic systems," Phys. Rev. Lett. **66**, 2172 (1991), and the reply by Bauer and Bertsch on the following page. The dependence of the decay laws on chaotic behavior is very general and has been considered in various contexts including room acoustics and the chaotic scattering of microwaves in an "elbow" cavity. Chaotic behavior is a sufficient, but not necessary condition for exponential decay.

Keith Briggs, "Simple experiments in chaotic dynamics," Am. J. Phys. **55**, 1083–1089 (1987).

S. N. Coppersmith, "A simpler derivation of Feigenbaum's renormalization group equation for the period-doubling bifurcation sequence," Am. J. Phys. **67** (1), 52–54 (1999).

J. P. Crutchfield, J. D. Farmer, and B. A. Huberman, "Fluctuations and simple chaotic dynamics," Phys. Repts. **92**, 45–82 (1982).

Robert DeSerio, "Chaotic pendulum: The complete attractor," Am. J. Phys. **71** (3), 250–257 (2003).

William L. Ditto and Louis M. Pecora, "Mastering chaos," Sci. Am. **262** (8), 78–82 (1993).

J. C. Earnshaw and D. Haughey, "Lyapunov exponents for pedestrians," Am. J. Phys. **61**, 401 (1993).

Daniel J. Gauthier, "Resource letter: CC-1: Controlling chaos," Am. J. Phys. **71** (8), 750–759 (2003). The article includes a bibliography of materials on controlling chaos.

Wayne Hayes, "Computer simulations, exact trajectories, and the gravitational N-body problem," Am. J. Phys. **72** (9), 1251–1257 (2004). The article discusses the concept of shadowing which is used in the simulation of chaotic systems.

Robert C. Hilborn, "Sea gulls, butterflies, and grasshoppers: A brief history of the butterfly effect in nonlinear dynamics," Am. J. Phys. **72** (4), 425–427 (2004).

Robert C. Hilborn and Nicholas B. Tufillaro, "Resource letter: ND-1: Nonlinear dynamics," Am. J. Phys. **65** (9), 822–834 (1997).

Ying-Cheng Lai, "Controlling chaos," Computers in Physics **8**, 62 (1994). Section 6.6 is based on this article.

R. B. Levien and S. M. Tan, "Double pendulum: An experiment in chaos," Am. J. Phys. **61** (11), 1038–1044 (1993).

V. Lopac and V. Danani, "Energy conservation and chaos in the gravitationally driven Fermi oscillator," Am. J. Phys. **66** (10), 892–902 (1998).

J. B. McLaughlin, "Period-doubling bifurcations and chaotic motion for a parametrically forced pendulum," J. Stat. Phys. **24**, 375–388 (1981).

Sergio De Souza-Machado, R. W. Rollins, D. T. Jacobs, and J. L. Hartman, "Studying chaotic systems using microcomputer simulations and Lyapunov exponents," Am. J. Phys. **58** (4), 321–329 (1990).

Bo Peng, Stephen K. Scott, and Kenneth Showalter, "Period doubling and chaos in a three-variable autocatalator," J. Phys. Chem. **94**, 5243–5246 (1990).

Bo Peng, Valery Petrov, and Kenneth Showalter, "Controlling chemical chaos," J. Phys. Chem. 95, 4957–4959 (1991).

Troy Shinbrot, Celso Grebogi, Jack Wisdom, and James A. Yorke, "Chaos in a double pendulum," Am. J. Phys. **60** (6), 491–499 (1992).

Niraj Srivastava, Charles Kaufman, and Gerhard Müller, "Hamiltonian chaos," Computers in Physics **4**, 549–553 (1990); ibid. **5**, 239–243 (1991); ibid. **6**, 84–88 (1992).

Todd Timberlake, "A computational approach to teaching conservative chaos," Am. J. Phys. **72** (8), 1002–1007 (2004).

Jan Tobochnik and Harvey Gould, "Quantifying chaos," Computers in Physics **3** (6), 86 (1989). There is a typographical error in this paper in the equations for step (3) of the algorithm for computing the Lyapunov spectrum. The correct equations are given in Project 6.18.

S. Warr, W. Cooke, R. C. Ball, and J. M. Huntley, "Probability distribution functions for a single particle vibrating in one dimension: Experimental study and theoretical analysis," Physica A **231**, 551–574 (1996). This paper and the book by Tufillaro, Abbott, and Reilly considers the motion of a ball bouncing on a periodically vibrating table. This nonlinear dynamical system exhibits fixed points, periodic and strange attractors, and period-doubling bifurcations to chaos, similar to the logistic map. Simulations of this system are very interesting, but not straightforward.

Tolga Yalcinkaya and Ying-Cheng Lai, "Chaotic scattering," Computers in Physics **9**, 511–518 (1995). Project 6.22 is based on a draft of this article. The map (6.40) is discussed in more detail in Yun-Tung Lau, John M. Finn, and Edward Ott, "Fractal dimension in nonhyperbolic chaotic scattering," Phys. Rev. Lett. **66**, 978 (1991).